INORGANIC CHEMISTRY
FRONTIERS

REVIEW

View Article Online
View Journal

Cite this: DOI: 10.1039/d5qi02301g

Phosphorescence emission from molecular complexes of bismuth

Katharina L. Deuter * and Rainer F. Winter

Received 18th November 2025,
Accepted 10th April 2026

DOI: 10.1039/d5qi02301g

rsc.li/frontiers-inorganic

Phosphorescent bismuth complexes are a class of materials that unite the unique photophysical properties of heavy (metal) elements with the advantages of low toxicity and affordability. Recent efforts in sustainable photochemistry, optoelectronics, and bioimaging have been focused on replacing the traditionally used rare and expensive platinum group elements with more sustainable alternatives such as bismuth. This review aims to clarify the photophysical processes relevant to Bi-based phosphors and to capture the recent progress in the development of luminescent molecular Bi complexes. We highlight general trends and provide insights into current challenges and Bi-specific issues.

Introduction

Excited triplet states are of pivotal importance in diverse fields ranging from physics to medicine. They find application in the transformation of visible light into chemical or electrical energy in photocatalytic conversion schemes,[1–3] in dye-sensitized solar cells (DSSCs), in photovoltaics,[3,4] and in the translation of electrical energy input into radiation output in organic or organometallic light-emitting diodes (OLEDs).[5–7] In a biomedical context, triplet states underlie the generation of oxidative stress due to singlet oxygen formation in photodynamic therapy or advanced bioimaging techniques.[8–10] All these applications rely on the ability of a photoactive ingredient (a sensitizer) to access the excited triplet manifold from an excited singlet state by efficient intersystem crossing (ISC) with the benefits of greatly enhanced excited-state lifetimes or being capable to sample all of the generated excitons, irrespective of their spin multiplicity.

Many of the above schemes utilize molecular metal complexes as the active component, typically of the middle to late 4d- and 5d-elements Re, Ru, Os, Ir, Pt, or Au.[5,11–16] These metal ions often provide the advantageous combinations of a large spin–orbit coupling constant ζ_{SOC}, thereby boosting ISC through the internal heavy atom effect, and endow the electronic excitations of their complexes with important charge-transfer contributions of the MLCT or LMCT type (MLCT = metal-to-ligand charge-transfer; LMCT = ligand-to-metal charge-transfer). Hosts of complexes of these noble metals with highly advantageous properties such as ISC with nearly unitarian quantum yields, long excited state lifetimes and suitability for the above-mentioned applications were devised and investigated.[17–21] However, their low natural abundance and unaffordable pricing present high obstacles as to their practical utilization in many of these schemes.

The surge of more viable alternatives has more recently brought the element Bi into focus. Bi has the highest spin–orbit coupling matrix element (ζ_{SOC} = 6381 cm^{-1}; Table 1) of all (practically) non-radioactive elements,[22,23] which makes Bi a candidate of choice for capitalizing on the internal heavy atom effect. Furthermore, Bi is often considered as non-toxic,[24,25] and as having "an excellent biosafety track record",[26] be it as the element or as its compounds. Several Bi compounds are indeed successfully administered for medical purposes,[26,27] and only occasional reports on irreversible adverse effects due to overdosing have appeared.[28–31] The problem of cytotoxicity is however aggravated in lipophilic

Table 1 List of elements with their atomic numbers and SOC constants[4]

Element	Atomic number	ζ_{SOC} (cm^{-1})
Ruthenium	44	1042
Rhodium	45	1259
Palladium	46	1504
Rhenium	75	2903
Osmium	76	3381
Iridium	77	3909
Platinum	78	4481
Gold	79	5104
Mercury	80	4270
Lead	82	5089
Bismuth	**83**	**6831**

Values were calculated for p, d electrons in an open shell of a neutral atom in the electronic ground state.[23]

Faculty for Chemistry, University of Konstanz, Universitätsstraße 10, 78457 Konstanz, Germany. E-mail: katharina.deuter@uni-konstanz.de, katharina.deuter@kit.edu

organobismuth compounds, as highlighted by studies on methylbismuthanes.[32,33] Bi has consequently made important appearances as a substitute of toxic lead ions in perovskites for solar cell applications,[34,35] and there are also many accounts on the use of Bi ions as dopants in solid-state emitter materials, often in concert with lanthanide ions or other solid-state emitter materials,[36,37] for anticounterfeiting[38–40] or in glasses for NIR emission.[41–43]

Despite the excellent prerequisites that the element Bi has for inducing ISC and the advances made in the fields of solid-state emitters, room-temperature phosphorescence (RTP) arising from molecular Bi complexes remains somewhat elusive. This review discusses photophysical processes observed for luminescent molecular Bi complexes in fluid solution or in a glassy frozen state. Extended inorganic solids, perovskite-type materials, and undefined nanoclusters are outside the scope of this article. The majority of molecular Bi emitters exhibit Bi in oxidation state +III and they therefore dominate this review, but we will also briefly discuss those few bismuth(I) and bismuth(V) emitters that have been reported in the literature.

Fundamental principles

Basic photophysical principles

Before we advance to discuss the individual types of phosphorescent Bi complexes and specific examples, it may be useful for some readers to pinpoint the processes by which excited triplet states can be generated from initially formed excited singlet states. Absorption of electromagnetic radiation in the ultraviolet (UV) and the visible (vis) regime by a molecule excites an electronic transition from the electronic singlet ground state S_0 into an electronic excited singlet state S_1 or a higher state S_n. Depending on the Franck-Condon factor, which is the extent by which nuclear coordinates of the ground and the respective excited state differ, electronic excitation also comes with the excitation of vibrational quanta on the excited state hypersurfaces. This and the possible, subsequent deactivation pathways of the excited electron are often summarized in a Jablonski diagram (Fig. 1). After internal conversion (IC), which is "an isoenergetic radiationless transition between two electronic states of the same multiplicity",[44] and vibrational relaxation, which is "the loss of vibrational excitation energy by a molecular entity through energy transfer to the environment caused by collisions",[44] into the vibrational ground state of electronic state S_1, fluorescence may occur according to Kasha's rule. Kasha's rule states that "polyatomic molecular entities luminesce with appreciable quantum yield only from the lowest excited state of a given multiplicity".[44] Fluorescence always competes with non-radiative decay, meaning "the disappearance of an excited species due to a radiationless transition" into S_0.[44] Another possible process emanating from an excited singlet state S_n is spin-forbidden ISC, which is "an isoenergetic radiationless transition between two electronic states having different multiplicities" to a triplet state T_m.[44] According to Hund's second rule, the excited state with the higher spin multiplicity has the lower electronic energy. ISC thus results in a vibrationally excited molecular entity in state T_m, which is then again subject to internal conversion of any triplet state higher than T_1 and vibrational relaxation, until it attains the vibrational ground state of state T_1. Emission from the latter state, which is phosphorescence, requires another quantum mechanically forbidden spin flip. This renders this process relatively slow and endows state T_1 with a lifetime in the microsecond (μs) to second (s) range, much longer than the typical nanosecond (ns) lifetime of fluorescence. Of course, phosphorescence emission has to compete with non-radiative decay pathways such as quenching by other triplet molecules or internal conversion.[22]

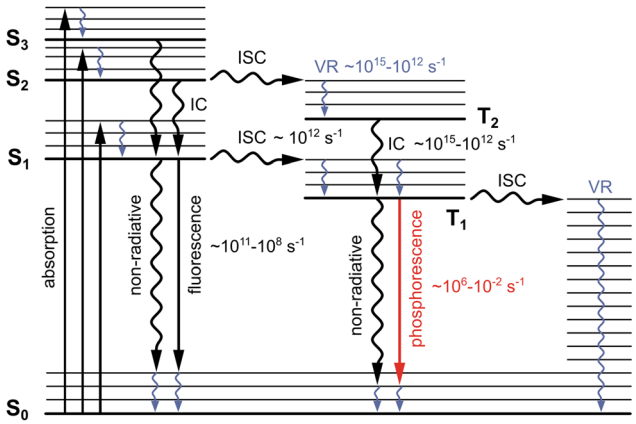

Fig. 1 Schematic representation of the photophysical processes of most molecules, represented in a simplified Jablonski diagram. Non-radiative processes are represented by wavy arrows while radiative processes are represented by straight arrows.

Spin–orbit coupling and intersystem crossing

ISC is essential for generating phosphorescence emission. Although this process is spin–forbidden, there are several ways to increase the probability of this transition. One of them is the so-called heavy atom effect (HAE), defined as "the enhancement of the rate of a spin-forbidden process by the presence of an atom of high atomic number, which is either part of or external to the excited molecular entity. Mechanistically, it corresponds to a spin–orbit coupling enhancement produced by a heavy atom".[44] As stated by this definition, one has to differentiate between the external and the internal HAE. The external HAE is based on the observation of enhanced singlet–triplet transitions even for molecules that do not contain a heavy atom, such as parent polyarenes, when embedded in solutions or in matrices of alkyl or aryl halides, with increasing efficiency in the order Cl < Br ≪ I.[45] The internal HAE describes the increased occurrence of ISC in a molecule to which a heavy atom is directly bonded by strong spin–orbit coupling (SOC).[46] Ågren and colleagues describe SOC as "the force which aims to "flip" the spin angular momentum (S) of an electron".[47] Mathematically,

it can be described by the spin–orbit Hamiltonian $\hat{H}_{SO}$ (eqn (1)),[47,48]

$$\hat{H}_{SO}=\frac{Ze^2}{2m_e{}^2c^2r^3}L\cdot S \quad (1)$$

where Z is the nuclear charge, L is the orbital angular momentum, S is the spin angular momentum, r is the orbital radius, e is the elementary charge of an electron, m_e is the electron mass and c is the speed of light under vacuum. Under the assumption of an initial singlet state denoted with Ψ_{S_a} and a final triplet state $\Psi_{T_b^\alpha}$ with fine structure levels α, the rate of ISC, k_{ISC}, can be written as given in eqn (2) in the Franck-Condon approach,

$$k_{ISC}=\frac{2\pi}{\hbar}\sum_{\alpha}\left|\left\langle\Psi_{T_b^\alpha}\middle|\hat{H}_{SO}\middle|\Psi_{S_a}\right\rangle\right|^2_{\{Q_0\}}\mathrm{FCWD} \quad (2)$$

where $\Psi_{T_b^\alpha}$ and Ψ_{S_a} are the total molecular wave functions of the final triplet and initial singlet states, respectively, while $\hbar$ is the reduced Planck constant, $\{Q_0\}$ denotes the geometry of the initial state at its energetic minimum, and FCWD refers to the Franck–Condon weighted density of final states at the energy of the initial state.[47,49,50] From the expressions in eqn (1) and (2) it becomes apparent that the rate of ISC is highly dependent on the nuclear charge Z. The dependence on Z at least partially explains why so many metal complexes with heavy atoms like Re, Au, Pt, Ir or Os show large ISC rates.[51,52] The ability of a metal atom or ion to promote ISC is given by its SOC constant ζ_{SOC}. Table 1 provides a list of selected elements with their atomic numbers and SOC constants.

While the ζ_{SOC} values imply that a heavier element will necessarily lead to larger spin–orbit interactions, Marian and colleagues note that relying on Z as a "rule of thumb [...] breaks down if the two states are close in energy".[49]

Under the assumption of small energy gaps between the involved electronic states, and of small relative horizontal displacements of the multidimensional potential energy surfaces of the involved electronic states, as well as the application of a harmonic oscillator as stated by Englman and Jortner,[53] the Franck–Condon weighted density (FCWD) of final states can be written as:[52]

$$\mathrm{FCWD}=\frac{1}{\sqrt{2\pi\hbar\omega_M\Delta E}}\exp\left(-\frac{\gamma\Delta E}{\hbar\omega_M}\right) \quad (3)$$

in which $\hbar$ is the reduced Planck constant, ω_M is the maximal vibrational frequency with nonvanishing displacement, ΔE is the adiabatic energy separation of the two involved potential energy surfaces, and γ is a structural parameter. With these conditions, the FCWD increases exponentially with decreasing ΔE, a condition commonly referred to as the 'energy gap law', and minimizing the energy difference ΔE between involved energetic states can thus lead to fast non-radiative rate constants.[52] The minimization of ΔE between a singlet and a triplet state can be achieved in multiple ways such as the formation of excimers, aggregates or polymers, or by spatial separation of the highest occupied molecular orbital (HOMO) and lowest unoccupied molecular orbital (LUMO) in donor–acceptor type species.[54–57] The latter design endows at least some of the relevant electronic excitations with a charge-transfer character. These approaches have unearthed efficient phosphorescence emitters of p-block main group elements, including Bi.[58,59] Charge-transfer (CT) excitation in metal complexes is usually classified according to the electron donor and the electron acceptor unit within the molecular entity. Four main types can be distinguished: metal-to-ligand charge-transfer (MLCT), ligand-to-metal charge-transfer (LMCT), intraligand charge-transfer (ILCT), where electron density is shifted from an electron-rich to an electron-poor segment of the same ligand, and ligand-to-ligand′ charge-transfer (LL′CT), where the metal ion serves to arrange an electron-rich ligand L and a σ- or π-acceptor ligand L′ in a fixed spatial and geometric arrangement. CT excitation is often accompanied by a more or less pronounced change in dipole moment due to the relocation of electron density. The absorption and emission wavelengths resulting from CT transitions can therefore show large dependencies on the polarity of the solvent.[60,61]

Radiative *vs.* non-radiative decay pathways

Once populated, an excited triplet state T_1 can return to the ground state S_0 not only by phosphorescence emission, but also by non-radiative deactivation pathways. Even in the absence of a direct crossing between different potential energy hypersurfaces, non-radiative decay from excited state S_1 or T_1 to ground state S_0 can occur through the overlap of wavefunctions between the zeroth vibrational level of state S_1 or T_1 and higher vibrational levels of the S_0 state of the same energy. This is followed by a rapid vibrational relaxation to the zeroth vibrational level of the S_0 state with the dissipation of thermal energy into the environment.[51,62] Vibrational relaxation is therefore accelerated when the energy gap between the involved states is shifted to lower energies, *i.e.* to the deep red or NIR regions, where fewer vibrational quanta of S_0 are required to be on par with the vibrational ground state of electronic states S_1 or T_1. This is dubbed as the energy-gap law.[49,53,63,64]

A further, radiationless decay mechanism is observed for compounds that emit in the NIR region of the spectrum, known as the inductive-resonant mechanism (IRM).[65] In the case of small electronic energy gaps, only a few vibrational overtones of solvent molecules may be of the same energetic level as the relevant excited state. This similarity in energy may then facilitate resonant coupling between the electronic transition of the compound and vibrational modes of nearby solvent molecules, dissipating the energy in the form of heat.[65]

Another pathway that may contribute to emission quenching is aggregation-caused quenching (ACQ). Noncovalent intermolecular interactions such as π-stacking may reduce the gap between the T_1 and S_0 states as well as enhance SOC, thereby causing radiationless decay.[66,67] On the other hand, aggregation may also boost the phosphorescence of aggregated forms of molecules which, as individuals, emit only weakly or not at

all. This is referred to as aggregation-induced emission (AIE) and usually relies on the blocking of non-radiative decay channels such as molecular rotations or vibrations in higher aggregates and the lowering of energetic differences between states.[54,68]

The influence of bismuth's oxidation state on the photophysical properties

General considerations for bismuth complexes

Bismuth complexes most commonly exhibit a Bi central ion in the oxidation state +III, but the oxidation states −I, +I, +II, +IV and +V have been reported as well.[69–71] To the best of our knowledge, no complexes in which Bi is assigned a formal oxidation state of −I, +II or +IV have been reported to be emissive so far and for this reason, they are excluded from this review.

The prevalence of the +III oxidation state is attributed to Bi's inert pair effect resulting from lanthanide contraction: because of poor shielding of the nuclear charge by the 4f atomic orbitals, the electrons residing in Bi's 6s atomic orbital are less shielded from the nucleus than the electrons within the 6p orbitals. This leads to an energetic stabilization of the 6s orbital and a large energetic difference to the 6p AOs.[70,72] As a result, the formation of hybrid orbitals becomes unfavourable and the AOs have predominant s- and p-characters, respectively.[73] At the same time, the inherent weakness of Bi-element bonds makes it difficult to compensate for the additional ionization energies required to empty the 6s orbital. The s-type lone pair is often referred to as being "stereochemically active", because it influences the coordination geometry and the bond angles between ligands that coordinate to bismuth(III) ions (*cf.* Fig. 2).[72,74–77]

Bi's position in the 6th period means that its atomic orbitals (AOs) are diffuse, polarizable and large and thus generally less capable of good overlap with those of other, lighter elements to form Bi–E bonds, where E = C; N; O; *etc*.[78–86] Consequently, Bi complexes may be prone to homolytic bond cleavage or dismutation.[87–95] This may be alleviated by employing multidentate ligands, which we explore briefly in the section Design strategies for emissive bismuth complexes.

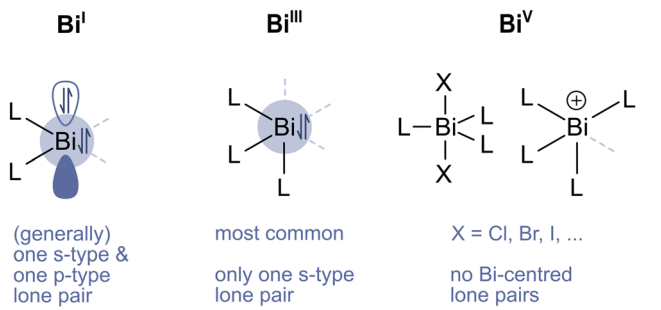

Fig. 2 Schematic representation of the lone pairs at Bi in the oxidation states +I, +III and +V. Note that for all compounds, other structures exist as well, and these are merely some of the most relevant for this review.

Thankfully, Bi compounds are easily capable of supporting multidentate ligands, and high coordination numbers (CNs) are rather common, even if the electron count at Bi then exceeds the octet rule.[74,96–99] In such instances, the compounds are referred to as being "hypervalent".[100] According to the octet rule, Bi^{X+} compounds are hypervalent whenever the CN is larger than $0.5(X + 3)$, meaning that bismuth(I) complexes with CN > 2, bismuth(III) complexes with CN > 3 and bismuth(V) complexes with CN > 4 are hypervalent. Often, Bi accommodates the extra electrons through the formation of 3-centre-4-electron bonds which it achieves particularly with halide, oxygen, sulphur or nitrogen ligands. A review by Hyvl gives an excellent overview of the basics and applications of hypervalent organobismuth complexes.[96]

Monomeric bismuth(I) complexes

Monomeric bismuth(I) complexes with a formal electronic configuration at Bi of $[Xe]4f^{14}5d^{10}6s^26p^2$ are generally highly reactive compounds with a singlet ground state, although exceptions with a triplet ground state have recently been reported in the literature.[101–103] Neutral, monomeric bismuth(I) compounds were long elusive until Dostál and colleagues reported a dimethindene stabilized by a tridentate ketimine-*N*,*C*,*N*-pincer type ligand in 2010.[104] These are stabilized by both σ-donation of imine lone pairs into the empty p-type orbital at bismuth(I), and steric protection of the bismuth(I) centre through bulky residues.[104–106] Without these or other coordinating ligands, bismuthinidene species tend to dimerize to species exhibiting Bi–Bi bonds.[105–107]

The energetically high-lying occupied Bi 6p orbital generally constitutes the major component to these compounds' HOMOs while the LUMO is often ligand-centred.[104,106,108–110] Thus, monomeric bismuth(I) complexes generally exhibit:

1. MLCT-type transitions in the visible region as their lowest-energy transition, with bismuth(I)'s occupied 6p-type lone pair as the donor MO and a ligand-centred MO as the acceptor orbital;

2. Metal-centred transitions between the occupied 6p or 6s type lone pair and one of the remaining, unoccupied 6p-type orbitals at Bi;

3. Intraligand or interligand transitions in which both the donor and acceptor MOs are ligand centred and reside at higher energies.

Bismuth(III) complexes

With a formal electron configuration of $[Xe]4f^{14}5d^{10}6s^2$, bismuth(III) complexes on the other hand exhibit only one lone pair of the s-type at Bi. Bismuth(III) complexes exhibit numbers of coordinating ligands ranging anywhere from two (for cationic complexes)[111] to nine.[112,113] The large coordination numbers and the hypervalency that bismuth(III) complexes may achieve arise from bismuth(III)'s Lewis acidity, specifically from its capability of forming 3-centre-4-electron bonds of σ- and π-type interactions with suitable donor ligands and its empty p-type orbitals.[96,98,100,114] Comprehensive reviews of the structures of Bi complexes with organic ligands were provided

by Silvestru or Sharutin and colleagues.[74,115] Overviews of the structures of cationic bismuth(III) complexes and organobismuth compounds have been provided by Lichtenberg and Gagnon and colleagues, respectively.[72,77] Due to the large diversity in coordination numbers, coordination modes and the variety of ligands that may bind to bismuth(III), all types of electronic transitions may be found for bismuth(III) complexes:

1. Metal-centred transitions, in which the s-type lone pair at bismuth(III) acts as the donor orbital, while the acceptor orbital consists of the empty p-type orbital at Bi, have been reported in the literature. Due to the large energy differences between the s-type lone pair and the p-type orbitals,[70,72,116] these transitions usually lie in the UV region.[117]

2. MLCT transitions in which the s-type lone pair at Bi acts as a donor orbital, while ligand-centred π* orbitals act as the acceptor orbitals.[118]

3. Transitions in which metal–halide bonding MOs act as the donor while other ligands are the acceptor units, sometimes referred to as MXLCT or XMLCT.[110,119]

4. LMCT type transitions, in which molecular orbitals localized on electron-rich ligands act as the donor orbitals and MOs consisting at least partially of empty p-type orbitals at bismuth(III) are the acceptor orbitals.[120,121]

5. LMXCT transitions, in which ligand MOs (usually high-lying π-type MOs at the ligands) are the donor while Bi–X antibonding interactions form the acceptor orbitals.[122,123]

6. LL′CT transitions, involving both donor and acceptor MOs residing on different ligands, usually of the n → π* or π → π* type.[124,125] If the donor ligand is a halide, these may be referred to as XLCT transitions.

7. Transitions occurring within one ligand. For ligands with extended π-systems, these transitions are generally of the π–π* type, but n → π* transitions are possible as well. These are often found at similar energies to transitions of the unbound ligands.[126,127]

With such a large diversity of observed types of electronic transitions, a general statement on the nature of the lowest-energy transition within bismuth(III) complexes is difficult, but overarching trends may be found for the general classes, which we will elucidate in the individual subsections in the section Classes of molecular Bi emitters. For now, it is important to remember that bismuth(III) complexes show a wide structural diversity and a large variety in possible electronic transition types.

Bismuth(V) complexes

In molecular complexes in which the central Bi ion exhibits the formal oxidation state of +V, and an electron configuration of $[Xe]4f^{14}5d^{10}$, Bi no longer possesses lone pairs of the s- or p-type. The lack of stereochemically active lone pairs means that the structures of organometallic bismuth(V) compounds may be predicted using the VSEPR model. In bismuthonium compounds in which CN = 4, bismuth(V) compounds generally exhibit a tetrahedral coordination environment, while trigonal bipyramidal and octahedral coordination environments are generally found for CN = 5 and CN = 6, respectively. As noted by Gagnon and colleagues, as well as Silvestru *et al.*,[72,74] a notable exception to this rule is presented by purple $Bi(Ph)_5$ which exhibits a square pyramidal coordination environment around Bi.

Lacking metal-centred lone pairs, bismuth(V) complexes generally do not exhibit electronic transitions in which the donor MO is metal-based. Thus, the observed electronic transitions for this class of compounds generally consist of

1. Intraligand transitions or
2. Interligand transitions of the n–π* or π–π* type
3. In combination with halide ligands, transitions may be observed in which ligand orbitals act the donor orbitals, while the metal–halide antibonding interactions act as the acceptor MOs, giving rise to LMXCT type transitions

Classes of molecular Bi emitters

In this section we will summarize the differing classes of molecular Bi emitters that have been investigated for their emission properties in solution or in glassy matrices at cryogenic temperatures. We have subdivided this section into bismuth(III), bismuth(I) and bismuth(V) compounds. The bismuth(III) emitters section is further divided into subsections (i) Bismuth halides, (ii) Triarylbismuthanes, (iii) Bismoles and bisimines, (iv) Hypervalent organometallic bismuth(III) compounds, (v) Bi complexes with Janus scorpionate and mercapto ligands, and (vi) Bi complexes with nitrogen donor and halide ligands. For solid-state and aggregation-induced emitters, we refer the reader to authoritative reviews by Rivard and Huang and colleagues.[59,128]

Bismuth(III) emitters

Bismuth halides. Bi halides are a naturally popular choice as starting materials of Bi complexes, and as such, many emissive Bi complexes contain halide ligands. This warrants a brief discussion of some of the simplest Bi halides. Solid-state emitters containing Bi halide anions have received some attention, and recent literature reviews on the luminescence properties of zero-dimensional metal halides have included an overview of the emissive properties of both fully inorganic and organic/inorganic Bi halides.[129,130] Other recent reviews focused on applications of Bi halide perovskites, including an overview of those that were investigated as white light-emitting diodes,[131] while the emissive properties of 0D-, 1D-, 2D- and 3D-based Bi perovskites were recently discussed in another review article.[132] A final review discussed the emissive properties of some compounds containing Bi-ate(III) anions or charged Bi_n clusters.[133]

The simple halogenido complexes $[BiCl_4]^-$ (**1**) and $[BiCl_6]^{3-}$ (**2**) possess metal-centred transitions in addition to LMCT transitions, in which an electron is promoted from the Bi 6s orbital to the empty 6p orbital. While the chloride compounds are reported to exhibit phosphorescence emission in MeCN solution at r.t., with values of λ_{phos} = 720 nm and λ_{phos} = 475 nm for **1** and **2** respectively,[117] their bromide analogues **3**

and **4** do not emit under the same conditions (*cf.* Table 2) and instead undergo photodecomposition leading to elemental Bi, Br_2 and $[Br_3]^-$.[92] Analogous observations of photoreactivity were made for the iodide compounds. The assumed decomposition pathway is attributed to the promotion of one electron from occupied MOs with Bi–X bonding or non-bonding contributions to unoccupied MOs consisting of antibonding interactions.[93] Studies on BiI_3 have revealed the underlying mechanism upon irradiation with UV light to be the dissociation into $BiI_2^{\bullet}$ and $I^{\bullet}$ radicals, which recombine to give BiI_3 or Bi and I_2.[94,95]

Moreover, Bi halides are often subject to distinct changes in colour upon cooling (thermochromism) due to changing Bi–X bond lengths.[122,134,135] Exemplarily, changes in the interatomic distances between Bi and iodide depending on the temperature were shown in a crystallographic study on compounds containing $[Bi_2I_9]^{3-}$ or $[Bi_3I_{11}]^{3-}$ anions and on BiI_3.[134]

Triarylbismuthanes. Table 3 summarizes the photophysical properties of representatives of this compound class. Perhaps the simplest class of triarylbismuthanes is composed of compounds with the general structure $BiAr^1Ar^2Ar^3$ in which three aryl substituents are bound to Bi. The bond angles between the aryl substituents generally assume values close to 90° (*cf.* top left of Fig. 3). This class of compounds generally displays ligand-centred transitions of a π–π* or n–π* character as their lowest-energy transitions. At r.t. in solution, most triarylbis-

Table 2 Summary of the emission properties of some of the simplest Bi halides

Ref.	Compound	Solution, r.t.
117	$[NEt_4]^+[BiCl_4]^-$ (**1**)	λ_{phos} = 720 nm Φ_{phos} = 1%
117	$[NEt_4]^+_3[BiCl_6]^{3-}$ (**2**)	λ_{phos} = 475 nm Φ_{phos} = 0.4%
92	$[NEt_4]^+[BiBr_4]^-$ (**3**)	n.o.[a]
92	$[NEt_4]^+_3[BiBr_6]^{3-}$ (**4**)	n.o.[a]

n.o. = not observed. [a] Photodegradation.

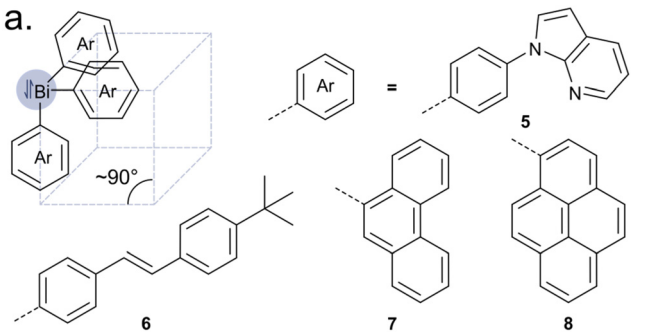

Fig. 3 Molecular structures of some triarylbismuthanes.

Table 3 Summary of the emission properties of triarylbismuthanes

Ref.	Nr.	Solution, r.t.	Solid, r.t.	Glassy matrix, 77 K	Solid, 77 K
136	**5**	λ_{flu} = 371 nm	λ_{phos} = 472 nm $\tau_{phos,1}$ = 0.368(9) ms $\tau_{phos,2}$ = 0.098(5) ms	λ_{phos} = 478 nm $\tau_{phos,1}$ = 0.577(8) ms $\tau_{phos,2}$ = 0.093(8) ms	λ_{phos} = 494 nm τ_{phos} = 0.209(1) ms
137	**6**	λ_{flu} = 375 nm $\lambda_{phos} \approx$ 400 nm[a]	—	—	—
138	**7**	λ_{flu} = 366 nm Φ_{flu} = 1.53%	λ_{flu} = 366 nm	—	—
140	**8**	$\lambda_{flu} \approx$ 380 nm λ_{flu} = 400–500 nm[b] Φ_{flu} = 0.44%	—	—	—
141	**9**	λ_{flu} = 395 nm τ_{flu} = n.r.	—	λ_{phos} = 423 nm $\tau_{phos,1}$ = 495 ms (63%) $\tau_{phos,2}$ = 2111 ms (37%)	—
126	**10**	λ_{flu} = 467 nm $\tau_{flu,1}$ = 59.0 ps (24%) $\tau_{flu,2}$ = 393 ps (76%) Φ_{flu} = 12%	λ_{flu} = 499 nm τ_{flu} = n.a. Φ_{flu} < 2%	λ_{phos} = 628 nm τ_{phos} = 1.11 ms	—
126	**11**	λ_{flu} = 379 nm $\tau_{flu,1}$ = 103 ps (83%) $\tau_{flu,2}$ = 597 ps (17%) λ_{phos} = 505 nm τ_{phos} = 61.5 ns $\Phi_{flu+phos}$ < 2%	λ_{flu} = 406 nm τ_{flu} = n.a. λ_{phos} = 487 nm τ_{phos} = n.a. (μs) $\Phi_{flu+phos}$ < 2%	λ_{phos} = 497 nm τ_{phos} = 724 μs	—
126	**12**	λ_{flu} = 391 nm $\tau_{flu,1}$ = 54.3 ps (94%) $\tau_{flu,2}$ = 1.39 ns (6%) λ_{phos} = 633 nm τ_{phos} = 8.43 μs $\Phi_{flu+phos}$ < 2%	λ_{flu} = 408 nm τ_{flu} = n.a. λ_{phos} = 628 nm τ_{phos} = n.a. (μs) $\Phi_{flu+phos}$ < 2%	λ_{phos} = 633 nm τ_{phos} = 399 μs	—

n.o. = not observed. [a] Shoulder speculated at a phosphorescence but not further confirmed. [b] Assigned as fluorescence by us.

muthanes are fluorescent with emission stemming from excited states localized on the aryl moieties.[136–141] The presence of Bi within these systems nevertheless leads to greatly reduced fluorescence quantum yields compared to the parent arenes, and from those few studies in which the authors also conducted measurements within the solid state or in frozen solutions, it becomes evident that the HAE of the Bi ion induces ISC and leads to the population of triplet states. The latter are generally ligand-centred and possess long lifetimes in the range of ms to seconds.[136,141] Exceptions to this were reported by Ohshita and colleagues (*vide infra*).[126] It should be noted that some of these compounds are reported to possess biexponential emission decay traces (*cf.* Table 3), which is usually an indication of aggregation or the presence of two emissive species.

An initial study reported on the emissive properties of *p*-(*N*-7-azaindolyl)phenyl compound **5** alongside its antimony and phosphorus homologs. **5** was shown to phosphoresce in frozen solutions of CH_2Cl_2 at 77 K in the blue/green region with λ_{phos} = 478 nm. Lifetimes for this emission lie in the millisecond regime with $\tau_{phos,1}$ = 0.577(8) ms and $\tau_{phos,2}$ = 0.093(8) ms, which is indicative of an aryl-centred triplet state. **5** is reported to be weakly fluorescent with an emission maximum at λ_{flu} = 371 nm at r.t. in CH_2Cl_2 solution.[136] TD-DFT calculations show that the underlying electronic transitions arise from (7-azaindolyl)phenyl-centred π–π* transitions with slight lone pair contributions from the respective pnictogen atom for the phosphorus and antimony compounds. While the authors state that TD-DFT calculations on **5** were inconclusive, it appears that the electronic transitions parallel those of the lighter congeners.[136]

Similar trends arise when a Bi compound **6** bearing three (*E*)-4-(4-*t*-butylstyryl)phenyl substituents (Fig. 3) is compared to its phosphorus, arsenic and antimony congeners. All pnictogen representatives were shown to be emissive in the violet region in degassed solutions of $CHCl_3$ at r.t. with λ_{flu} = 375 nm and a shoulder emission at λ_{phos} = 400 nm, which the authors attribute to phosphorescence, although no emission decay traces were reported. Their attribution is based instead on the finding that the shoulder increases in relative intensity in the order P < As < Sb < Bi in qualitative agreement with the HAE along this series.[137] Ligand-centred violet emission from π–π* states at λ_{flu} = 366 nm is also observed for **7** bearing phenanthryl ligands.[138] The blue-shifted UV-vis spectra of **7** compared to those of its P to Sb analogues indicates a decrease in the contribution of the pnictogen atom. In addition, a decrease in the quantum yield of **7** is reported to occur with Φ_{flu} = 2.52% for Pn = P, Φ_{flu} = 3.6% for Pn = Sb, and Φ_{flu} = 1.53% for **7**.[138]

The tris(pyrenyl)-substituted compound **8** was reported to fluoresce at $\lambda_{flu} \approx$ 380 nm in CH_2Cl_2 at r.t. Additionally, a second red-shifted emission at *ca.* λ = 400–500 nm is observed for **8** and its lighter congeners which the authors attribute to the presence of static excimers, or ground state aggregates, as the ratio between the two emission features changes with the irradiation wavelength. This suggests that the emission stems from two different species.[140] In lieu of emission lifetimes, it remains unclear if the low-energy emission stems from an excited triplet state or whether this is a fluorescence emission, as was reported for related, pyrene-modified compounds reported in 2024 (*vide infra*).[89,142] The similarity in the emission wavelength and the wavelengths of the fluorescence emissions of aggregates of the compounds reported by Winter and colleagues at λ_{flu} = 432 nm and λ_{flu} = 500 nm[142] speaks for fluorescence.

Two studies focused on the combination of Bi with triarylboron structural motifs. The first study, stemming from 2019, reports on the emission of **9** (*cf.* Fig. 4), which is fluorescent at λ_{flu} = 395 nm at r.t., and phosphorescent at 77 K at λ_{phos} = 423 nm. The exceptionally long lifetimes of $\tau_{phos,1}$ = 495 ms (63%) and $\tau_{phos,2}$ = 2111 ms (37%) are indicative of triplet states localized on the organic residues, as stated by the authors.[141]

Exceptions to the general observation of exclusively fluorescence emission at r.t. in solution were provided by Ohshita and colleagues in 2024.[126] Here, the emissive behaviour of several Bi thiophenyl compounds **10–12**, with or without an attached boron acceptor, is reported. At r.t. in CH_2Cl_2 solution, **11** and **12** are dually emissive with λ_{phos} = 633 nm for **12** and λ_{phos} = 505 nm for **11** and lifetimes of τ_{phos} = 8.43 μs and τ_{phos} = 61.5 ns, respectively. For **10**, the authors observed pure fluorescence emission at r.t. and phosphorescence only at cryogenic temperatures in 2-MeTHF. The long lifetime of τ_{phos} =

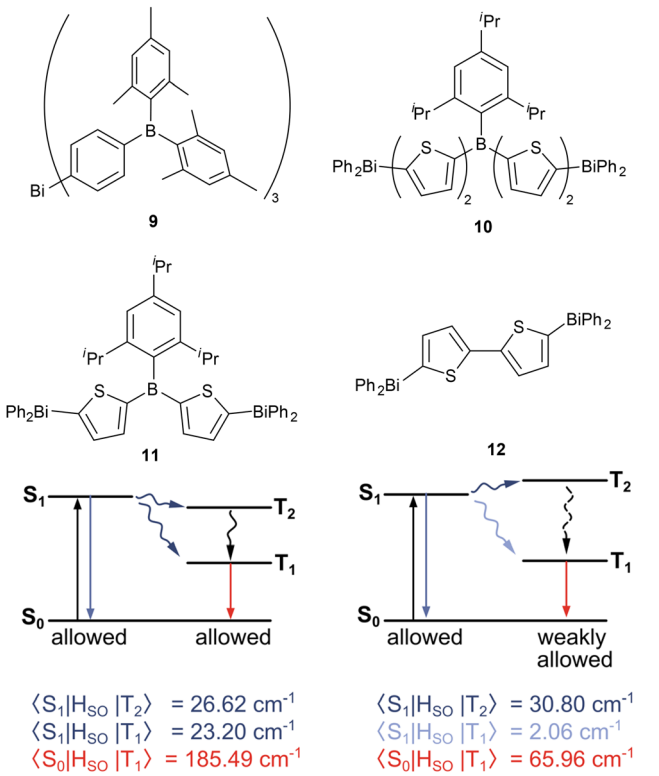

Fig. 4 Molecular structures of compounds **9–12** and simplified Jablonski diagrams including calculated spin–orbit coupling constants (SOCCs) for two compounds displaying dually emissive behaviour at r.t. in solution.

1.11 ms and the absence of phosphorescence at r.t. indicate an organic moiety-centred emission and considerable quenching effects at r.t. In solutions cooled to 77 K, **11** and **12** are also phosphorescent with somewhat shorter lifetimes of τ_{phos} = 724 μs and τ_{phos} = 399 μs, respectively. Interestingly, the corresponding organic moiety present in complex **11** is also phosphorescent at 77 K with nearly identical, albeit more finely resolved emission and with a considerably longer phosphorescence lifetime of τ_{phos} = 280 ms. This supports ligand-centred emission with Bi providing an external HAE, thereby accelerating radiative decay by increasing k_{phos}. The lower lifetimes of **11** and **12** are attributed to larger SOC between the T_1 and S_0 states, which is reflected by the calculated spin–orbit coupling constants (SOCCs) of 185.49 cm^{-1} for **11** and 65.96 cm^{-1} for **12** compared to 30.82 cm^{-1} for **10**. The authors also suggest that ISC occurs between states S_1 and energetically higher states T_n based on their calculations of energy levels and SOCCs between S_0–S_2 and T_1–T_5. These circumstances are shown schematically at the bottom of Fig. 4 for **11** and **12**.

Bismoles and bisimines. Another class of triarylbismuthanes that has been under focus for use as emissive materials is that containing bismole units or fused Bi-containing heterocycles.[58,125,127,143–148] Some of these compounds have been featured previously in review articles by Ito and colleagues,[149] and by Rivard and colleagues.[150] The electronic transitions within these systems usually consist of π–π* transitions within the aromatic backbone or interligand charge-transfer transitions.[125] As for the triarylbismuthanes in the previous section, most of these are fluorescent or non-emissive at r.t. in solution, and the contribution of the Bi ion is most apparent in their low fluorescence quantum yields (*cf.* Table 4).[127,143,146–148] Investigations of these compounds' emissive behaviour at 77 K or within the solid state often show phosphorescence emission, indicating Bi-mediated ISC and the population of triplet states that deactivate non-radiatively at r.t. in solution. In the solid state, several other bismole compounds or polymers were reported to be phosphorescent due to aggregation-induced emission.[58,151]

The Bi congener of 9-phenylcarbazole, **13**, which is perhaps the simplest of the bismoles reported within this section, was investigated alongside its N, P, As and Sb analogues by Inaba *et al.* in 2017. It should be noted that the heavier congeners of

Table 4 Summary of the emission properties of triarylbismuthanes with bismole or bisimine units

Ref.	Nr.	Solution, r.t.	Solid, r.t.	Glassy matrix, 77 K
143	**13**	$\lambda_{flu} \approx 330$ nm[a] $\tau_{flu,1}$ = 21.4 ns $\tau_{flu,2}$ = 3.2 ns	—	λ_{phos} = 489 nm τ_{phos} = 1.2 ms
148	**14**	λ_{flu} = 310–330 nm	—	λ_{phos} = 454 nm τ_{phos} = 0.26 ms
125	**15**	λ_{phos} = 550 nm (Air)/545 nm (Ar) τ_{phos} = 0.12 μs (Air)/0.13 μs (Ar) Φ_{phos} = 2.45%	λ_{phos} = 618 nm τ_{phos} = 61.06 μs Φ_{phos} = 0.22%	—
125	**16**	λ_{phos} = 575 nm (Air)/550 nm (Ar) τ_{phos} = 0.12 μs (Air)/4.60 μs (Ar) Φ_{phos} = 4.50%	λ_{phos} = 647 nm τ_{phos} = 32.43 μs Φ_{phos} = 0.20%	—
125	**17**	λ_{phos} = 580 nm (Air)/574 nm (Ar) τ_{phos} = 0.16 μs (Air)/2.50 μs (Ar) Φ_{phos} = 2.27%	λ_{phos} = 673 nm τ_{phos} = 15.93 μs Φ_{phos} < 0.10%	—
125	**18**	λ_{phos} = 590 nm (Air)/587 nm (Ar) τ_{phos} = 0.27 μs (Air)/1.02 μs (Ar) Φ_{phos} = 2.06%	λ_{phos} = 674 nm τ_{phos} = 4.80 μs Φ_{phos} < 0.10%	—
127	**19**	$\lambda_{flu} \approx 400$ nm λ_{phos} = 622 nm τ_{phos} = n.d. Φ_{phos} = 0.2%	$\lambda_{flu} \approx 400$ nm	—
127	**20**	$\lambda_{flu} \approx 400$ nm λ_{phos} = 625 nm τ_{phos} = 5.2 μs Φ_{phos} = 0.2%	λ_{phos} = 620 nm	—
127	**21**	$\lambda_{flu} \approx 400$ nm λ_{phos} = 635 nm τ_{phos} = 6.3 μs Φ_{phos} = 0.2%	λ_{phos} = 617 nm	—
127	**22**	$\lambda_{flu} \approx 400$ nm λ_{phos} = 601 nm τ_{phos} = 2.1 μs Φ_{phos} = 0.2%	$\lambda_{flu} \approx 400$ nm	—
146	**23**	λ_{flu} = 658 nm Φ_{flu} = 3.9%	—	—
147	**24**	λ_{flu} = 634 nm Φ_{flu} = 3.3%	—	—

n.d. = not determined. [a] Value estimated from graphs, as not provided by authors.

N-arylcarbazoles were much earlier reported by Davydov and Godik *et al.* These authors have reported that on descending the group from P to As, Sb and Bi, the phosphorescence quantum yield increased at the expense of fluorescence, paralleled by a decrease in phosphorescence lifetime, but no further details from these studies are, unfortunately, available to us.[152–154] The later Inaba study indicated that all representatives of this group are fluorescent in 2-MeTHF solution at r.t. with $\lambda_{flu} \approx 330$ nm. TD-DFT calculations show that the respective pnictogen atom has little contribution to the HOMO. A slight heteroatom contribution to the LUMO is observed for the heavier elements P, As, Sb and Bi, and accordingly, phosphorescence is observed for solutions in 2-MeTHF at 77 K for all compounds with the exception of the phosphorus analogue.[143]

Similar results were found for the dipyridinobismole compound **14** with r.t. fluorescence and phosphorescence exclusively in the glassy matrix at 77 K.[148] TD-DFT calculations show that for **14**, the HOMO and LUMO are both localized on the bipyridyl unit so that the majority of the energetically low-lying electronic excitations are π–π* transitions.[125] Despite the large similarity of the molecular structures of **14** and compounds **15–18**, the latter compounds were reported to be phosphorescent at r.t. in MeCN solution. The emission maxima of the bismoviologens **15–18** in Fig. 5 range from $\lambda_{phos} = 550$ nm to $\lambda_{phos} = 590$ nm, depending on the substituents (refer to Table 4), with quantum yields ranging from $\Phi_{phos} = 2.06\%$ for **18** to $\Phi_{phos} = 4.50\%$ for **16**.[125] TD-DFT calculations show that for these compounds, the HOMO resides on the phenyl substituent while the LUMO is localized on the viologen unit, thus rendering the HOMO–LUMO transition of a LL′CT character. Despite the lack of direct bismuth(III) involvement in the electronic transition with the lowest energy, the proximal HAE of the Bi ion is sufficient to accelerate ISC and induce the population of a ligand-centred excited triplet state.[125] For other systems, it has been observed that such segregation of the HOMO and LUMO leads to the enhancement of ISC, a feature often explored in the design of organic TADF emitters.[155–157] Unsurprisingly, the emission of **15–18** is solvent dependent, with more polar solvents leading to red-shifted emission.[125]

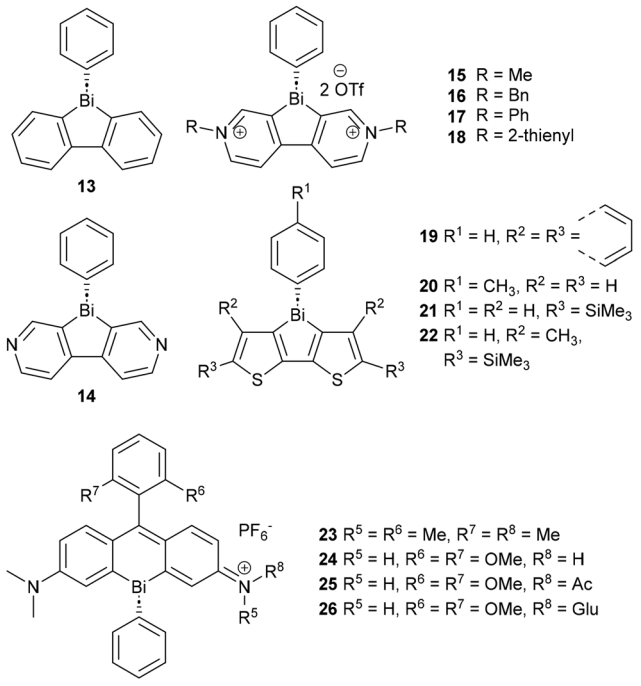

Fig. 5 Molecular structures of triarylbismuthanes featuring bismole units which were investigated for their luminescence properties in solution or glassy matrices.

Further examples of RTP in solution, accompanied by weak fluorescence, were reported by Ohshita and colleagues in 2010 for dithienobismoles **19–22** as shown in Fig. 5. These were reported to be dually emissive in $CHCl_3$ solution at r.t. with λ_{phos} = 601–635 nm and quantum yields of $\Phi_{phos} = 0.2\%$. Lifetimes range from $\tau_{phos} = 2.1$ μs to 6.3 μs, depending on the substituents, and are compiled in Table 4. TD-DFT calculations show a very slight Bi participation to the LUMO, which may facilitate the population of excited triplet states. **21** and **22**, bearing trimethylsilyl groups at the R^3 position, additionally exhibit solid-state phosphorescence while the other two representatives of this class are only fluorescent under the same conditions. This difference was attributed to the prevention of quenching effects through π-stacking in the solid state through the bulky -$SiMe_3$ groups. Dilute solutions of these compounds were unfortunately proven to be unstable.[127]

Incorporation of a Bi ion into the scaffold of the common dye rhodamine leads to a compound **23** (Fig. 5) that is emissive in the red region with $\lambda_{flu} = 658$ nm and possesses a quantum yield of $\Phi_{flu} = 3.9\%$ in 2-[4-(2-hydroxyethyl)piperazin-1-yl]ethanesulfonic acid (HEPES) buffer solutions with dimethyl sulfoxide as a cosolvent. Despite the lack of phosphorescence, **23** possesses a non-emissive triplet state, as evidenced by the generation of $^1O_2$. Irradiating cancer cells that were previously treated with **23** hence led to a significant increase in cell death.[146] Degradation studies show that **23** is susceptible to decomposition upon irradiation at 625 nm. A second study reported on two further asymmetrically substituted Bi rhodamine derivatives **24** and **25**. They possess similar photophysical properties to **23** (*cf.* Table 4), although **25** does not show the $^1O_2$ generation. Adding the γ-glutamyl (Glu) group to the established scaffold yielded a non-emissive complex **26** that could be used to generate the emissive and $^1O_2$ producing species **24** through the enzymatic activity of γ-glutamyl transpeptidase (GGT). The phototoxicity of the **24** species generated from **26** in GGT-active cell lines was confirmed in cell experiments.[147]

Hypervalent, organometallic bismuth(III) compounds. Organometallic Bi complexes with additional, coordinating heteroatoms such as N or O incorporated in anionic tridentate *N*,*C*,*N* and *O*,*N*,*O* pincer or bidentate *N*,*C* and *N*,*O* ligands, often in combination with halide ligands X^- have been another recent focus of study. In these hypervalent species, coordination of neutral donors or bonding to halides gives rise to 4-electron-3-centre bonds which provide the basis for tran-

sition types with metal contributions (MLCT, LMCT, XMLCT, and MLXCT) or the involvement of differing ligands (LL′CT). These compounds, summarized in Fig. 6 and 7, are united by reasonable stability towards moisture, though not always towards light. A large number of these compounds are fluorescent at r.t. and dually emissive or phosphorescent at 77 K, although RTP arising from ligand-centred triplet states has been reported for some representatives of this group as well. With the presence of heteroatoms, some of these compounds are prone to aggregation and therefore to aggregation-induced emission (AIE). Multiexponential decay traces dominate in this class of compounds (refer to Table 5), indicating the presence of several (different) species or aggregation numbers. Despite the similarity of, in particular, the *N*,*C*,*N* pincer complexes, the overall emissive behaviour of this class of compounds is rather diverse.

The first reports of the emissive behaviour of bismuth complexes with *N*,*C*,*N*-ligands stems from a 2024 study. 7-Coumarinyl *N*,*C*,*N* pincer complexes such as **28** and **30** are non-emissive at r.t. but show green phosphorescence in 2-MeTHF at 77 K.[89] Bi *N*,*C*,*N* complexes bearing 1-pyrenylthiolate ligands such as **27** and **29** are dually emissive under the same conditions, with phosphorescence emission stemming from aggregates of the pyrenyl moieties. All four compounds

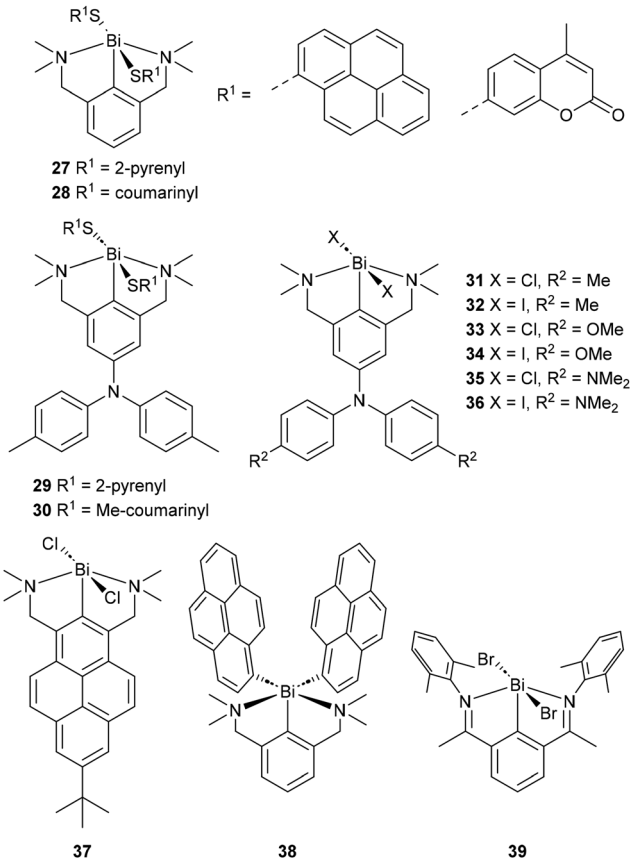

Fig. 6 Molecular structures of pentacoordinate organometallic bismuth complexes with tridentate *N*,*C*,*N* pincer ligands.

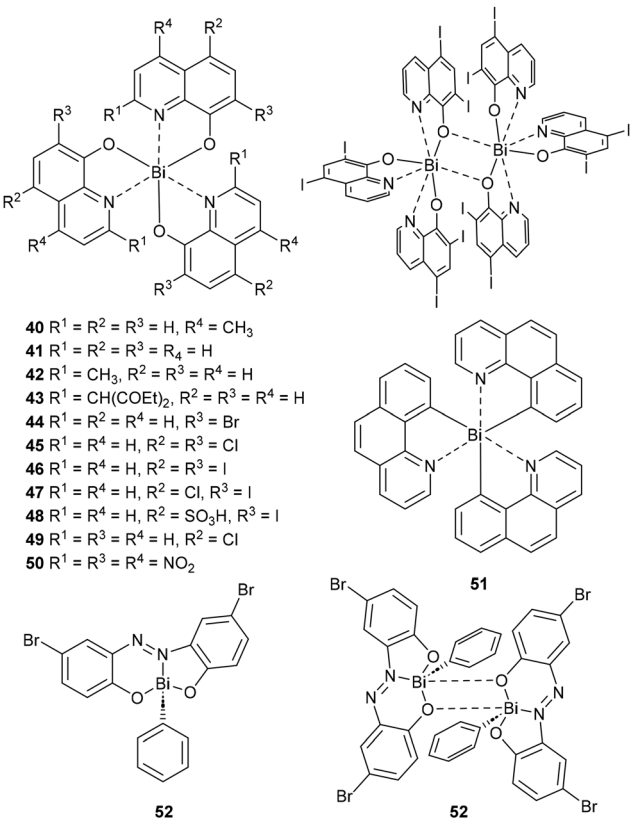

Fig. 7 Molecular structures of hypervalent Bi complexes with anionic chelating ligands featuring neutral imine donors.

are unfortunately light-sensitive and decompose under irradiation at r.t. in solution under release of the corresponding disulfide.[89] The tendency towards aggregation-induced emission from pyrenyl-substituted Bi compounds matches well with a previous literature report.[140]

When the thiolate ligands are exchanged for halides to give compounds **31–36** these compounds are fluorescent at r.t. in solution with triarylamine centred emission, and those compounds bearing methyl groups at the triarylamine additionally display aggregation-induced fluorescence.[124] At 77 K, those complexes with R^2 = –Me or –OMe display phosphorescence in addition to the fluorescence emission (Table 5). Interestingly, the fluorescence to phosphorescence ratio of compounds **31–34** is solvent-dependent with increased phosphorescence in less polar solvents. Changes of the excitation spectra for the two emissions indicate that aggregation increases the intensity of the phosphorescence emission at the expense of fluorescence. Accordingly, solid-state samples of the *p*-tolyl (R^2 = –Me) and *p*-anisyl (R^2 = –OMe) complexes **31–34** are phosphorescent in the orange to red region at r.t. while **35** and **36** with –NMe_2 substituents remain non-emissive. The fluorescence and phosphorescence quantum yields decrease in each instance with Φ_{phos} (X = Cl) > Φ_{phos} (X = I) (compare the values for pairs **31** & **32**, **33** & **34** and **35** & **36** in Table 5).[124] This observation agrees with literature reports on Bi halide emitters

Table 5 Summary of the emission properties of hypervalent bismuth emitters with multidentate ligands and neutral N-donors

Ref.	Nr.	Solution, r.t.	Solid, r.t.	Glassy matrix, 77 K	Solid
89	**27**	—	—	λ_{flu} = 387 nm λ_{phos} = 640 (aggr.) $\tau_{flu,1}$ = 26 ns (26%) $\tau_{flu,2}$ = 5.3 ns (66%) $\tau_{flu,3}$ = 16 ns (8%) $\tau_{phos,1}$ = 276 μs (30%) (aggr.) $\tau_{phos,2}$ = 453 μs (70%) (aggr.)	—
89	**28**	—	—	λ_{phos} = 504 $\tau_{phos,1}$ = 18 μs (21%) $\tau_{phos,2}$ = 51 μs (66%) $\tau_{phos,3}$ = 141 μs (13%)	—
89	**29**	—	—	λ_{flu} = 387 nm λ_{phos} = 641 (aggr.) $\tau_{flu,1}$ = 2.4 ns (49%) $\tau_{flu,2}$ = 10 ns (44%) $\tau_{flu,3}$ = 37 ns (7%) $\tau_{phos,1}$ = 152 μs (27%) (aggr.) $\tau_{phos,2}$ = 485 μs (73%) (aggr.)	—
89	**30**	—	—	λ_{phos} = 509 $\tau_{phos,1}$ = 33 μs (43%) $\tau_{phos,2}$ = 79 μs (52%) $\tau_{phos,3}$ = 224 μs (5%)	—
124	**31**	λ_{flu} = 379 nm λ_{flu} = 506 nm (aggr.) $\tau_{flu,1}$ = 1.9 ns (47%) $\tau_{flu,2}$ = 6.6 ns (53%) $\tau_{flu,1}$ = 2.4 ns (62%) (aggr.) $\tau_{flu,2}$ = 8.7 ns (38%) (aggr.) Φ_{flu} < 0.1%	λ_{phos} = 634 nm $\tau_{phos,1}$ = 0.14 μs (59%) $\tau_{phos,2}$ = 0.96 μs (41%) Φ_{phos} = 1.3%	λ_{flu} = 445 nm λ_{phos} = 585 nm $\tau_{flu,1}$ = 2.3 ns (81%) $\tau_{flu,2}$ = 9.7 ns (19%) $\tau_{phos,1}$ = 5.6 μs (58%) $\tau_{phos,2}$ = 20 μs (42%) Φ_{flu} = 28% Φ_{phos} = 47%	—
124	**32**	λ_{flu} = 381 nm λ_{flu} = 505 nm (aggr.) $\tau_{flu,1}$ = 2.2 ns (28%) $\tau_{flu,2}$ = 6.5 ns (72%) $\tau_{flu,1}$ = 2.8 ns (45%) (aggr.) $\tau_{flu,2}$ = 9.9 ns (55%) (aggr.) Φ_{flu} < 0.1%	λ_{phos} = 653 nm $\tau_{phos,1}$ = 61 μs (72%) $\tau_{phos,2}$ = 2.0 μs (28%) Φ_{phos} < 0.1%	λ_{flu} = 446 nm λ_{phos} = 612 nm $\tau_{flu,1}$ = 2.4 ns (80%) $\tau_{flu,2}$ = 9.6 ns (20%) $\tau_{phos,1}$ = 12 μs (36%) $\tau_{phos,2}$ = 21 μs (64%) Φ_{flu} = 2% Φ_{phos} = 29%	—
124	**33**	λ_{flu} = 389 nm $\tau_{flu,1}$ = 0.55 ns (6%) $\tau_{flu,2}$ = 4.9 ns (94%) Φ_{flu} < 0.1%	λ_{phos} = 612 nm $\tau_{phos,1}$ = 0.29 μs (44%) $\tau_{phos,2}$ = 1.0 μs (56%) Φ_{phos} = 0.9%	λ_{flu} = 447 nm, λ_{phos} = 611 nm, $\tau_{flu,1}$ = 3.1 ns (67%) $\tau_{flu,2}$ = 9.6 ns (33%) $\tau_{phos,1}$ = 12 μs (87%) $\tau_{phos,2}$ = 31 μs (13%) Φ_{flu} = 3% Φ_{phos} = 47%	—
124	**34**	λ_{flu} = 393 nm $\tau_{flu,1}$ = 0.85 ns (5%) $\tau_{flu,2}$ = 4.9 ns (95%) Φ_{flu} < 0.1%	λ_{phos} = 710 nm $\tau_{phos,1}$ = 0.59 μs (70%) $\tau_{phos,2}$ = 1.8 μs (30%) Φ_{phos} = 0.2%	λ_{flu} = 450 nm λ_{phos} = 655 nm $\tau_{flu,1}$ = 1.9 ns (39%) $\tau_{flu,2}$ = 4.4 ns (61%) $\tau_{phos,1}$ = 6.4 μs (42%) $\tau_{phos,2}$ = 15 μs (58%) Φ_{flu} = 0.3% Φ_{phos} = 14%	—
124	**35**	λ_{flu} = 429 nm $\tau_{flu,1}$ = 2.2 ns (82%) $\tau_{flu,2}$ = 9.0 ns (18%) Φ_{flu} < 0.1%	n.o.	λ_{flu} = 466 nm λ_{phos} = 700 nm[a] $\tau_{flu,1}$ = 2.5 ns (57%) $\tau_{flu,2}$ = 9.2 ns (43%) Φ_{flu} = 1.3%	—
124	**36**	λ_{flu} = 431 nm $\tau_{flu,1}$ = 2.3 ns (53%) $\tau_{flu,2}$ = 9.0 ns (47%) Φ_{flu} < 0.1%	n.o.	λ_{flu} = 477 nm λ_{phos} = 670 nm[a] $\tau_{flu,1}$ = 2.2 ns (60%) $\tau_{flu,2}$ = 7.7 ns (40%) Φ_{flu} = 0.3%	—
142	**37**	λ_{flu} = 405 nm λ_{flu} = 500 nm (aggr.) $\tau_{flu,1}$ = 17 ns (15%) $\tau_{flu,2}$ = 59 ns (85%) Φ_{flu} = 2.4%	—	λ_{flu} = 379 nm λ_{flu} = 485 nm (aggr.) λ_{phos} = 610 nm $\tau_{flu,1}$ = 20 ns (40%) $\tau_{flu,2}$ = 59 ns (60%)	—

Table 5 *(Contd.)*

Ref.	Nr.	Solution, r.t.	Solid, r.t.	Glassy matrix, 77 K	Solid
				$\tau_{phos,1}$ = 2.0 ms (97%) $\tau_{phos,2}$ = 10 ms (3%)	
142	**38**	λ_{flu} = 393 nm λ_{flu} = 432 nm (aggr.) λ_{phos} = 610 nm (aggr.) $\tau_{flu,1}$ = 2.5 ns (84%) $\tau_{flu,2}$ = 20 ns (13%) $\tau_{flu,3}$ = 132 ns (3%) τ_{flu} = 2.5 ns (aggr.) $\tau_{phos,1}$ = 0.10 ms (58%) (aggr.) $\tau_{phos,2}$ = 0.21 ms (42%) (aggr.) Φ_{flu} = 8.1% Φ_{flu} = 17.3% (aggr.) Φ_{phos} = 0.9% (aggr.)	—	λ_{flu} = 371 nm λ_{flu} = 397 nm (aggr.) λ_{phos} = 595 nm (aggr.) $\tau_{flu,1}$ = 2.3 ns (95%) $\tau_{flu,2}$ = 13 ns (4%) $\tau_{flu,3}$ = 150 ns (1%) τ_{phos} = 4.6 ms (aggr.)	—
110	**39**	n.o.	n.o.	λ_{phos} = 500 nm τ_{phos} = 376 μs	λ_{phos} = 560 nm
158	**40**	—	—	λ_{flu} = 469 nm λ_{phos} = 667 nm Φ_{flu} = 4.1% $\Phi_{phos} \leq 0.1\%$	—
159	**41**	λ_{flu} = 540 nm τ_{flu} < 0.5 ns $\Phi_{flu} \approx 0.06\%$ $\lambda_{phos} \approx 650$ nm $\tau_{phos} \approx 2$ μs Φ_{phos} < 0.01% λ_{flu} = 415 nm	—	λ_{flu} = 495 nm τ_{flu} < 20 ns λ_{phos} = 625 nm τ_{phos} = 80 μs	—
160	**42**	λ_{flu} = 540 nm (dimer)	—	—	—
160	**43**	λ_{flu} = 423 nm Φ_{flu} < 0.01%	—	—	—
160	**44**	λ_{flu} = 440 nm λ_{flu} = 525 nm (dimer) Φ_{flu} = 0.013% (dimer)	—	—	—
160	**45**	λ_{flu} = 371 nm λ_{flu} = 520 nm (dimer) Φ_{flu} = 0.03% (dimer)	—	—	—
160	**46**	λ_{flu} = 393 nm λ_{flu} = 542 nm (dimer) Φ_{flu} < 0.01% (dimer)	—	—	—
160	**47**	λ_{flu} = 390 nm λ_{flu} = 526 nm (dimer) Φ_{flu} < 0.01% (dimer)	—	—	—
160	**48**	λ_{flu} = 467 nm λ_{flu} = 530 nm (dimer) Φ_{flu} = 0.01% (dimer)	—	—	—
160	**49**	λ_{flu} = 380 nm Φ_{flu} = 9.0%	—	—	—
160	**50**	λ_{flu} = 484 nm Φ_{flu} = 0.01%	—	—	—
118	**51**	λ_{phos} = 520 nm $\tau_{phos,1}$ = 35 μs $\tau_{phos,2}$ < 0.2 μs Φ_{phos} = 10(3)%	—	—	—
161	**52**	$\lambda_{flu} \approx 640$ nm[a] (dmso) $\lambda_{flu} \approx 675$ nm[a] (toluene)	$\lambda_{flu} \approx 590$ nm[a] $\tau_{flu} \approx 15$ ns[a]	—	—

n.o. = not observed. [a] Value estimated from graphs, as not provided by authors.

(*vide infra*).[92,93,117] Oxidation of the dimethylamine-substituted representatives **35** and **36** delivers compounds that are weakly fluorescent in the NIR, with emission emanating from triarylamine$^{+\bullet}$-centred doublet states.[124]

Phosphorescence in solution stemming from aggregates is also observed for Bi complexes **37** and **38** with direct 1-pyrenyl attachment, both at r.t. and at 77 K. Like **8**,[140] **37** and **38** are robust towards continuous irradiation. There is however an unexpected difference between them: while the aggregation of **37** with only one pyrenyl unit leads to fluorescence, the complex **38** bearing two pyrenyl ligands displays phosphorescence stemming from aggregates in addition to fluorescence.[142] TD-DFT calculations assign both fluorescence and phosphorescence emissions to ligand-centred π–π* transitions

within these molecules with no Bi contributions to the involved MOs,[89,124,142] and the observation of fluorescence in conjunction with phosphorescence at 77 K matches reports on other organometallic Bi compounds.[126,141,143,148]

The last representative of this compound class, **39**, shown at the bottom right of Fig. 6, follows the trend of ligand-centred emission. **39** is emissive at cryogenic temperatures both in the solid state and in glassy matrices of 2-MeTHF with λ_{phos} = 500 nm and λ_{phos} = 560 nm, respectively. Large energy differences between λ_{exc} and λ_{phos} of ΔE = 7930 cm^{-1} as well as DFT calculations on **39** indicate a considerable structural difference between the T_1 and S_1 states. The non-emissive behaviour at r.t. is therefore attributed to quenching through structural rearrangements. It is assumed that the promotion of an electron from a HOMO with a partial Bi–X_2 4-electron-3-centre bond character to a ligand-centred excited state cleaves one of the Bi–X bonds. In quantum chemical calculations, the angle Br1–Bi1–Br2 is 171.7° for the singlet ground state and is reduced to 92.5° for the excited triplet state.[110]

Several other reports focus on hexacoordinate Bi complexes with bidentate chelating ligands. An interesting case of contradictory results spanning nearly 50 years of research is presented with reports on trioxinate complexes such as **41** and derivatives, whose structures are compiled in Fig. 7 and whose emission properties are summarized in Table 5.[158–160] An initial study conducted in 1965 on **40** alongside its main group (Al, In, and Pb) and 3d transition metal element congeners (Zn, Mn, Cu, Cd, Ni, Cr, Fe, and Co) reported green fluorescence accompanied by red phosphorescence in matrices of EtOH at 77 K.[158] A second study, conducted 20 years later, reported ligand-centred green fluorescence at λ_{flu} = 540 nm and a very weak, red phosphorescence that is better observed at 77 K for **41**.[159] The assumption of green fluorescence and red phosphorescence remained unchallenged until 2013, when a systematic study of Bi complexes bearing differently substituted oxyquinolate ligands **42–50** by Trogler and colleagues revealed that the green fluorescence stems from dimers, shown exemplarily for **46** at the top right of Fig. 7, which formed already at low concentrations. The monomers were instead found to be fluorescent in the violet region due to ligand-centred transitions.[160] While the authors of the Trogler study focused solely on the green fluorescence, and make no mention of a red phosphorescence, it appears plausible that the earlier-reported red emission also arises from dimers.

For the Bi complex **51**, which possesses three coordinating, bidentately chelating benzo[*h*]quinoline ligands, the coordination through the nitrogen donors destabilises the s-type lone pair at bismuth so that this complex displays a partially metal-centred HOMO while the unoccupied MOs are centred on the ligands.[118] This makes **51** one of the very few organometallic Bi complexes compiled in this article with an MLCT character to its lowest-energy transition. **51** emits at λ_{phos} = 520 nm with a biexponential emission decay trace with lifetimes of τ_{phos} = 35 μs and <0.2 μs (Table 5). With a value of Φ_{phos} = 10(3)%, it displays the largest phosphorescence quantum yield of a Bi compound in solution at r.t. reported to date. The authors argue that it is precisely the Bi involvement in the HOMO–LUMO transition that is crucial for efficient ISC and phosphorescence emission. Excitation spectra recorded at differing wavelengths show that the ratio of short-lived and long-lived components to the emission is excitation wavelength-dependent. It should be noted that this observation as well as the observation of biexponential emission decay traces may be rooted in aggregation, as was found in other reports.[89,124,140,142,160] Unfortunately, this compound is sensitive to light and decomposes within only a few seconds if irradiated at $\lambda_{exc} \leq$ 390 nm.[118]

Reported by Tanaka and colleagues in 2023, Bi compound **52** is fluorescent at r.t. and at 77 K. Solutions of **52** in dimethyl sulfoxide or toluene fluoresce with $\lambda_{flu} \approx$ 640 nm or $\lambda_{flu} \approx$ 675 nm. A significant blue shift of the emission is observed at 77 K in 2-MeTHF with $\lambda_{flu} \approx$ 590 nm, and a lifetime which we estimate to lie in the range of $\tau_{flu} \approx$ 15 ns supports the assignment of the emission as fluorescence, which is also consistent with the small Stokes shift.[161] Consistent with the report on weak r.t. fluorescence are the calculations on **52** which show that the lowest-energy excitation exclusively involves π–π* transitions on the azobenzene unit. Somewhat surprising is the lack of a phosphorescence emission at 77 K, as **52** is the only Bi complex with imine chelates that is not reported to phosphoresce at 77 K.[161]

Bi complexes with Janus scorpionate and mercapto ligands. In 2013 and 2014, Mitzel and colleagues reported on the luminescence properties of several Bi complexes bearing Janus scorpionate and mercaptodiazole, -triazole and -tetrazole ligands, shown in Fig. 8.[162–165] Some of these compounds are weakly emissive at r.t., but become luminescent when cooled to 77 K. The emission is attributed largely to ligand-centred triplet states and, in some cases, metal-centred transitions. However, a lack of quantum chemical calculations and often of emission decay traces makes it difficult to rationalize the origin of the emission or even its character. None appears to display RTP in solution, and it appears that the structurally flexible coordination environment around Bi allows for non-radiative decay.

Exemplarily, the bimetallic complex **53** bearing scorpionate ligands is emissive in CH_2Cl_2 solution at r.t. with λ_{flu} = 485 nm. While a lack of emission decay traces makes exact assignment difficult, it is tentatively assumed to be fluorescence. At cryogenic temperatures, the emission feature of **53** becomes structured with several separate maxima, which may indicate dual emission with fluorescence at λ_{flu} = 441 and λ_{phos} = 482 nm. The authors speculate that the origin of the emission is either a metal-centred sp or LMCT transition.[162]

The two complexes **54** and **55** phosphoresce at 77 K in glasses of ethanol with emission at λ_{phos} = 459 nm and λ_{phos} = 552 nm, and lifetimes of τ_{phos} = 16.1 ms and τ_{phos} = 0.33 ms, respectively (Table 6). In addition to this phosphorescence, **55** also possesses fluorescence features at λ_{flu} = 456 nm. For **54**, the emission is assumed to stem from a ligand-centred triplet state based on the similarity to the emission of the corresponding sodium salt of the ligand. For **55**, the authors assume

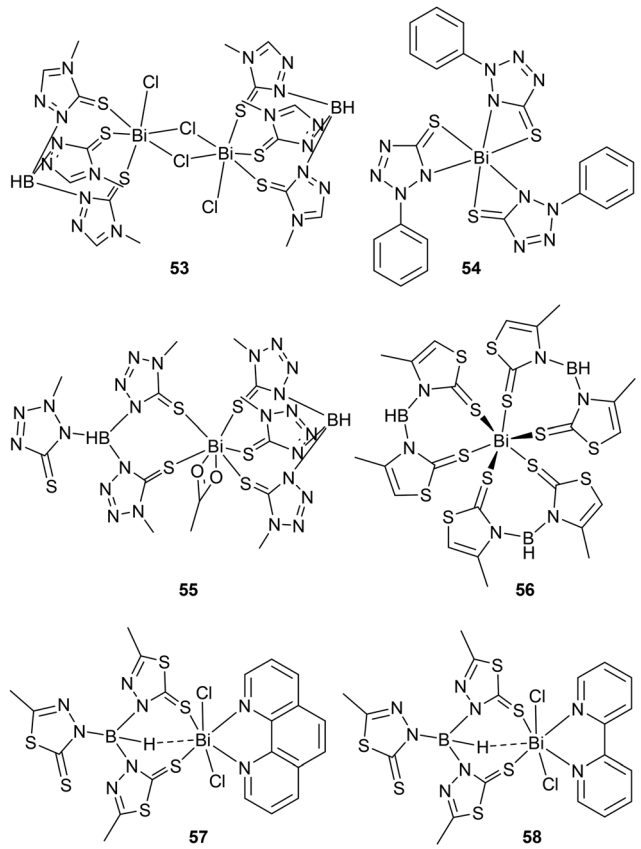

Fig. 8 Molecular structures of Bi complexes with Janus scorpionate ligands investigated for their emissive behaviour in solution or glassy matrices.

Table 6 Summary of the emission properties of Bi complexes with Janus scorpionate ligands

Ref.	Nr.	Solution, r.t.	Solid, r.t.	Glassy matrix, 77 K
162	**53**	λ_{flu} = 485 nm[a]	—	λ_{flu} = 441[b] λ_{phos} = 482 nm[b]
163	**54**	n.o.	—	λ_{phos} = 459 nm τ_{phos} = 16.1 ms
163	**55**	n.o.	—	λ_{flu} = 456 nm λ_{phos} = 552 nm τ_{phos} = 0.33 ms
165	56	n.o.	λ_{phos} = 674 nm	λ_{phos} = 618 nm
164	**57**	n.o.	—	λ_{phos} = 466 nm τ_{phos} = 3.35 ms
164	**58**	n.o.	—	$\lambda_{flu,1}$ = 449 nm $\lambda_{flu,2}$ = 487 nm λ_{phos} = 553 nm τ_{phos} = 0.37 ms

n.o. = not observed. [a] Assigned as fluorescence by us. [b] Not entirely clear whether fluorescence or phosphorescence due to missing emission decay traces.

a metal-centred sp state to be the source of the phosphorescence emission while its fluorescence is assumed to arise from a ligand-centred excited state.[163] The long lifetime of this phosphorescence emission however points rather to a CT or ligand-centred state. **56** is reported to possess metal-centred transitions that are low in energy and the complex emits in the red region at λ_{phos} = 674 nm at r.t. in the solid state and at λ_{phos} = 618 nm and 77 K in ethanol glass.[165] The compounds **57** and **58** are emissive at 77 K in EtOH solution with ligand-centred phosphorescence.[164] The latter assignment is based on the similarity of this emission to compounds with phen- and bipy-centred excited triplet states in multiple other studies which combine Bi and phen or bipy, in which phosphorescence emission arises from ligand-centred triplet states.[113,166–168] Lifetimes in the millisecond range confirm the phosphorescent nature of the emission with τ_{phos} = 0.37 ms and τ_{phos} = 3.35 ms, respectively (refer to Table 6). The authors argue that the lack of Bi participation is the reason for the long lifetimes and lack of room-temperature phosphorescence. It is argued that in the presence of low-lying ligand-centred π-acceptor orbitals, ligand-centred transitions are favoured over the transitions with metal contributions observed for their other Janus scorpionate complexes.[164]

Bi complexes with nitrogen donor and halide ligands. Many common dyestuffs such as dipyrromethenes akin to boron-dipyrromethenes (BODIPYs), corroles, or porphyrins,[169–171] which belong to the most popular organic photocatalysts, contain pyrrolic units. As such, it is of no surprise then that several studies have combined Bi with pyrrolide ligands (refer to Fig. 9 and 10 for their structures).[172–175] These electron-rich

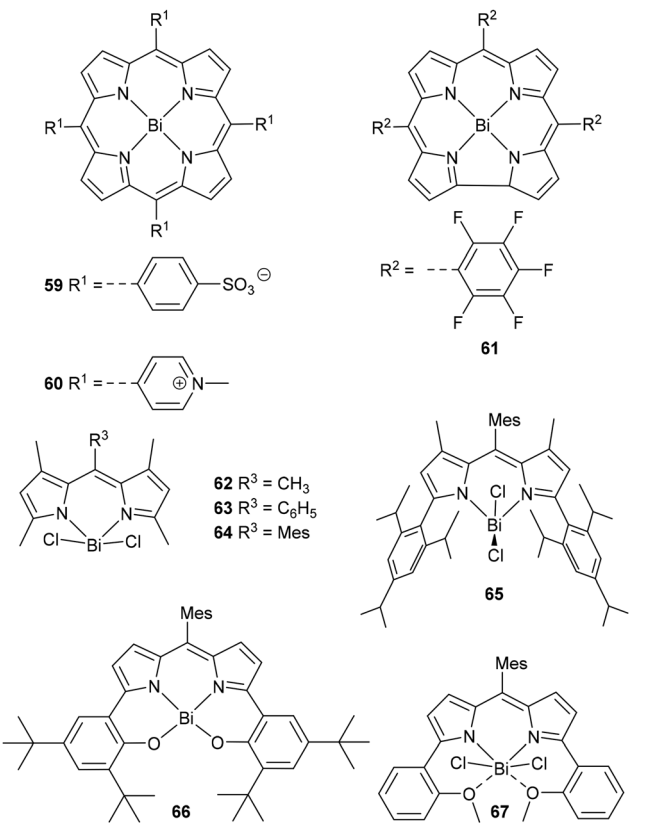

Fig. 9 Molecular structures of Bi complexes with corrole, dipyrromethene or porphyrin ligands.

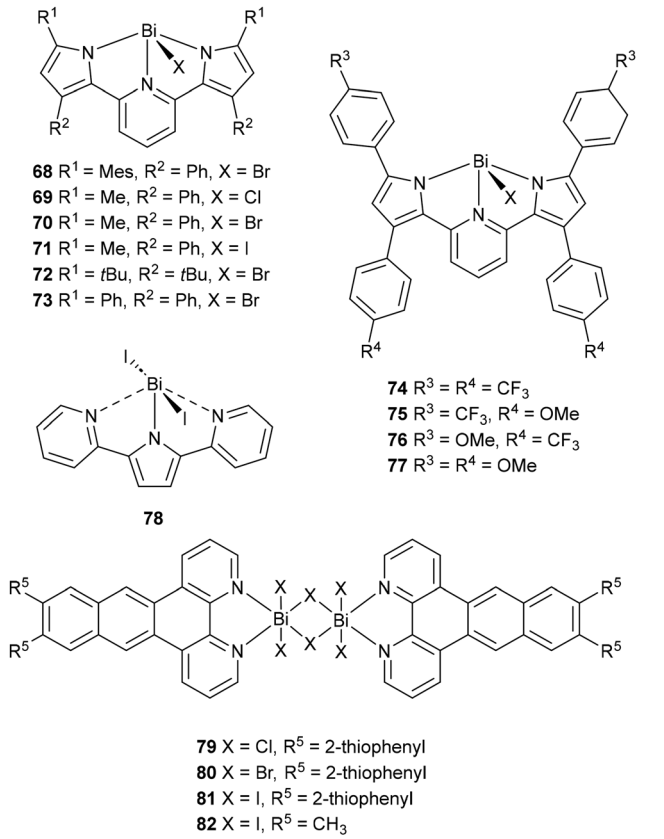

Fig. 10 Molecular structures of Bi complexes with pyrrolic, pyridine and phenanthrene ligands.

ligands generally possess high-lying, occupied MOs while at the same time providing rigid coordination environments as bi-, tri- or tetradentate chelates. Within this class of compounds, those compounds which exhibit intraligand π–π* transitions as their lowest-energy excitation are weakly fluorescent at r.t. while those with LMXCT transitions as their lowest-energy transition are non-emissive at r.t. but phosphorescent at 77 K (refer to Table 7). Some of these compounds were reported to be highly sensitive toward moisture.

Corroles and porphyrins are common structural motifs for photocatalysts and often display intriguing properties such as anti-Kasha emission and very short emission lifetimes.[179,180] The combination of the Bi^{3+} ion with the often-used porphyrin backbone has yielded two water-soluble Bi metalloporphyrins **59** and **60** (see Fig. 9) which emit at r.t. in water, both from the S_2 and S_1 states.[174] In accordance with a ligand-centred emission, the emission spectra of both complexes upon excitation are vibronically resolved with transitions occurring from the S_1 state to vibrational levels of the S_0 state $S_0(\nu = 0)$, $S_0(\nu = 1)$ and $S_0(\nu = 2)$, resulting in emission maxima in the red region with λ_{flu} = 609 nm, 657 nm and 714 nm for **59** and at λ_{flu} = 636 nm, 672 nm, and 730 nm for **60**. Lifetimes support fluorescence emission with τ_{flu} = 3.18 ns and 1.38 ns, respectively. The emission from the S_2 state lies in the blue region with λ_{flu} = 427 nm, 451 nm for **59** and at λ_{flu} = 459 nm and 486 nm for **60**. The emission spectra of both complexes are blue-shifted and possess diminished quantum yields in comparison with their free ligands, pointing at distortion of the porphyrin ligand, with a more substantial effect on the S_2 state. While no solid-state structures are reported within this study, literature reports on other Bi porphyrins show that the Bi ion resides out of the coordination plane with d(Bi–N) ≈ 2.32–2.34 Å and the porphyrin ligand is slightly dome-shaped to accommodate the Bi ion.[181–184] Other studies report on the use of a non-emissive Bi corrole complex **61** as a suitable photosensitizer for the generation of singlet oxygen.[175]

Combining the dipyrromethene motif with other central ions or with heavy halogen atoms is a commonly pursued strategy when attempting to occupy the non-emissive triplet states within these systems for $^1O_2$ generation.[185–187] The Bi representatives of this class of compounds are fluorescent in solution at λ_{flu} = 535 nm for **62**,[172] or at λ_{flu} = 568 nm for **65** (for structures, see Fig. 9),[173] with sharp emission profiles and small Stokes shifts reminiscent of those commonly observed for BODIPYs. TD-DFT analyses on these compounds reveal that the electronic transitions arise from ligand-centred π–π* transitions and that the heavy atom makes only a minor contribution.[172,173] Hinting at the population of a non-emissive triplet state, very low quantum yields of Φ_{flu} = 0.2% were recorded for **65**, while a larger value of Φ_{flu} = 6.6% was found for the related Sb compound.[173] Indeed, in a later study on Bi and Sb complexes with a N_2O_2-type tetradentate dipyrrin ligand, as is found for **66**, the Sb compound showed a quantum yield of Φ_{flu} = 0.8% while the Bi compound "did not exhibit notable photoluminescence emission".[176] Mirroring results were found for compound **67** and its Sb counterpart, in which the latter possesses a fluorescence quantum yield of Φ_{flu} = 5%, compared to Φ_{flu} = 0.2% for **67**. Unfortunately, the Bi compounds **62–64** that do not bear sterically shielding substituents at the BODIPY are prone to rapid decomposition in solution, but the coordination of additional oxygen donors, either in N_2O_2 motifs (**66**)[176] or through adeptly placed –OMe groups (**67**),[177] alleviates the issue.

A number of reports by the Winter group focused on the emission properties of Bi complexes **68–77** with pyridine-dipyrrolide ligands (Fig. 10). These electron-rich ligands endow the complexes with high-lying ligand-centred π-orbitals, while at the same time the Bi–X units provide antibonding orbitals centred on the Bi–X bonds such that these are involved in the LUMO with Bi contributions of ∼30%. It was hypothesized that the involvement of Bi in the LUMO would enhance ISC by endowing energetically low-lying electronic transitions with a partial CT character. Accordingly, the dipyrrolide complexes **68–77** are phosphorescent in 2-MeTHF solution at 77 K with an emission wavelength range of λ_{phos} = 602 nm–645 nm, depending on the substituents, with lifetimes in the short microsecond range, and quantum yields of up to Φ_{phos} = 18.5% (*cf.* Table 7).[29,110] Varying the halide has no influence on the emission wavelengths and only shortens the excited state lifetimes from X = Cl to I in accordance with the increasing HAE along the halides (compare values in Table 7). Upon

Table 7 Summary of the emission properties of bismuth coordination compounds with pyrrolic or pyridine and halide ligands

Ref.	Nr	Solution, r.t.	Solid, r.t.	Glassy matrix, 77 K	Solid, 77 K
174	**59**	λ_{flu} (S_1) = 609, 657, 714 nm λ_{flu} (S_2) = 427, 451 nm τ_{flu} (S_1) = 3.18 ns τ_{flu} (S_2) = 580 fs[a] Φ_{flu} (S_1) = 1.94% Φ_{flu} (S_2) = 0.0790%	—	—	—
174	**60**	λ_{flu} (S_1) = 636, 672, 730 nm λ_{flu} (S_2) = 459, 486 nm τ_{flu} (S_1) = 1.38 ns τ_{flu} (S_2) = 187 fs[a] Φ_{flu} (S_2) = 0.0199% Φ_{flu} (S_1) = 1.92%	—	—	—
175	**61**	n.o.	—	—	—
172	**62**	λ_{flu} = 535 nm	—	—	—
173	**65**	λ_{flu} = 568 nm Φ_{flu} = 0.2%	—	—	—
176	**66**	n.o.	—	—	—
177	**67**	λ_{flu} = 590 nm Φ_{flu} = 0.2%	—	—	—
122	**68**	n.o.	n.o.	λ_{phos} = 606 nm $\tau_{phos,1}$ = 190 μs (49%) $\tau_{phos,2}$ = 81 μs (51%)	—
122	**69**	n.o.	n.o.	λ_{phos} = 610 nm $\tau_{phos,1}$ = 479 μs (4%) $\tau_{phos,2}$ = 153 μs (96%)	—
122	**70**	n.o.	n.o.	λ_{phos} = 622 nm $\tau_{phos,1}$ = 224 μs (59%) $\tau_{phos,2}$ = 73 μs (41%)	—
122	**71**	n.o.	n.o.	λ_{phos} = 614 nm $\tau_{phos,1}$ = 219 μs (48%) $\tau_{phos,2}$ = 59 μs (52%)	—
122	**72**	n.o.	n.o.	λ_{phos} = 640 nm $\tau_{phos,1}$ = 166 μs (18%) $\tau_{phos,2}$ = 55 μs (82%)	—
122	**73**	n.o.	n.o.	λ_{phos} = 645 nm $\tau_{phos,1}$ = 39 μs (20%) $\tau_{phos,2}$ = 14 μs (80%)	—
178	**74**	n.o.	n.o.	λ_{phos} = 602 nm $\tau_{phos,1}$ = 65 μs (56%) $\tau_{phos,2}$ = 35 μs (44%) Φ_{phos} = 18.5%	—
178	**75**	n.o.	n.o.	λ_{phos} = 621 nm $\tau_{phos,1}$ = 74 μs (31%) $\tau_{phos,2}$ = 33 μs (69%) Φ_{phos} = 3.9%	—
178	**76**	n.o.	n.o.	λ_{phos} = 640 nm $\tau_{phos,1}$ = 57 μs (24%) $\tau_{phos,2}$ = 25 μs (76%) Φ_{phos} = 1.7%	—
178	77	n.o.	n.o.	λ_{phos} = 641 nm $\tau_{phos,1}$ = 123 μs (13%) $\tau_{phos,2}$ = 51 μs (87%) Φ_{phos} = 1.1%	—
123	**78**	n.o.	n.o.	λ_{phos} = 589 nm τ_{phos} = 128 μs Φ_{phos} = 50.8%	—
93	**79**	λ_{flu} = 468 nm $\tau_{flu,1}$ = 0.11 ns (28%) $\tau_{flu,2}$ = 0.42 ns (73%) Φ_{fl} = 1.62%	—	—	—
93	**80**	λ_{flu} = 467 nm $\tau_{flu,1}$ = 0.12 ns (13%) $\tau_{flu,2}$ = 0.42 ns (87%) Φ_{fl} = 0.98%	—	—	—
93	**81**	λ_{flu} = 469 nm $\tau_{flu,1}$ = 0.2 ns (15%) $\tau_{flu,2}$ = 0.43 ns (85%) Φ_{flu} = 0.56%	—	—	—

n.o. = not observed. [a] Estimated by the Strickler–Berg equation.

lowering the temperature, these compounds' UV-Vis spectra are significantly blue-shifted by up to 1360 cm^{-1}, a phenomenon that is observable to the naked eye with colour impression changing from violet to red.[110] This thermochromism points at a rather flexible coordination environment, which is assumed to render them non-emissive at r.t. in solution. In spite of the lack of room-temperature emission of this class of compounds, it is nevertheless promising for the design of phosphorescent materials as the large Bi contribution renders ISC fast enough to outcompete fluorescence.

Exchanging the pyridine-dipyrrolide for the dipyridine-pyrrolide ligand yields the complex **78** (Fig. 10) that also possesses an LMXCT character within its lowest-energy transition. **78** was investigated alongside the Sb and As representatives. All three compounds are phosphorescent in 2-MeTHF solutions at cryogenic temperatures, although not at r.t. Quantum yields of Φ_{phos} = 50.8% for **78** and a lack of fluorescence emission indicate an efficient population of the excited triplet state. Large structural rearrangements, confirmed by TD-DFT calculations and the large Stokes shift, however seem to quench emission at r.t. This compound was shown to generate singlet oxygen in low yields upon irradiation despite not possessing an emissive triplet state at r.t. Interestingly, despite the increase of the heavy atom effect along the series from As to Sb to Bi, the arsenic representative possesses the shortest phosphorescence lifetime. This was attributed to a better overlap between the ligand-centred ground state and metal–halide-centred excited states due to the shorter ligand–metalloid bond lengths.[123]

In 2024, Schroeder and colleagues reported on the emissive behaviour of the three Bi complexes **79–82**, shown in Fig. 10, of which **79–81** showed ligand-centred fluorescence at r.t, in DMF or MeCN solutions, with lifetimes in the range of nanoseconds (refer to Table 7), while **82** was prepared to better understand the UV-vis absorptive properties of **81** and not investigated for its luminescence properties. Photoluminescence measurements in solvents of differing polarity (DMF *vs.* MeCN) show a slight red shift of the emission with increasing solvent polarity, hinting at a slight CT character of the underlying transition. Measurements in mixtures of DMF/H_2O showed aggregation-induced emission for those complexes containing Br^- or I^- ligands and this might be the source of the multiexponential emission decay traces observed for these compounds (see also Table 7).[93] Transient absorption spectroscopy reveals an excited ligand-centred triplet state at r.t. at ~500 nm that is non-emissive with a lifetime of 5.5 μs, 2.2 μs and 7.1 μs for **79**, **80**, and **81**, respectively.[93]

Bismuth(I) emitters (bismuthinidenes)

Bismuthinidenes, *i.e.* Bi complexes with the metal ion in the oxidation state +I, present an interesting perspective and opportunity in the sense that these usually highly reactive complexes possess, in addition to the Bi 6s lone pair, an additional p-type lone pair at Bi. Bismuthinidenes most commonly possess a singlet ground state with the HOMO localized almost entirely on the bismuth(I) ion. As such, the lowest-energy transition in these systems is usually of the MLCT type. In 2025, the Winter and Cornella groups reported nearly simultaneously on the emissive behaviour of *N*,*C*,*N*-modified bismuth(I) complexes **83**[110] and **84**[188] which possess a singlet ground state consisting largely of a Bi centred p-type lone pair. Both complexes display NIR r.t. phosphorescence in solution. The combination of a small T_1–S_0 energy difference and large degrees of SOC, confirmed by TD-DFT calculations on **83**, and emission localized in the NIR region of the spectrum lead to short phosphorescence lifetimes of τ_{phos} = 5.2 ns for **83** for the 960 nm emission at r.t. (Table 8). The *tert*-butyl-substituted compound **84** emits at λ_{phos} = 795 nm, with very similar non-radiative rate constants, lifetimes and quantum yields to those of **83**. Transient absorption spectroscopy conducted on **84** shows a very rapid ISC process within 2.2 ps for this system.[188] For both compounds, the quantum yields are low at $\Phi_{phos} = 5 \times 10^{-3}$% and $\Phi_{phos} = 3 \times 10^{-3}$% for **83** and **84**, respectively, and non-radiative transitions appear to be the major deactivation pathway. In which form the energy is instead dissipated is unclear, but structural rearrangements, non-radiative decay due to the energy gap law, or the transfer of energy to the solvent by way of resonant coupling (IRM) are all plausible pathways (refer to the section Radiative *vs.* non-radiative decay pathways under Fundamental principles).

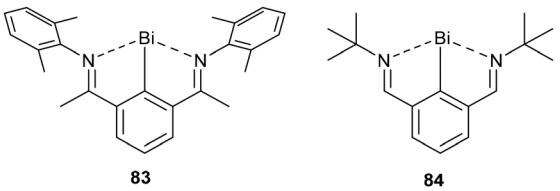

83 **84**

Fig. 11 Molecular structures of emissive bismuth(I) compounds.

Table 8 Summary of the emission properties of bimuthinidene bismuth(I) phosphors

Ref.	Nr.	Solution, r.t.	Solid, r.t.	Glassy matrix, 77 K
110	**83**	λ_{phos} = 960 nm τ_{phos} = 5.2 ns $\Phi_{phos} = 5 \times 10^{-3}$%	λ_{phos} = 970 nm	λ_{phos} = 960 nm $\tau_{phos,1}$ = 121 ns (66%), $\tau_{phos,2}$ = 215 ns (33%)
188	**84**	λ_{phos} = 795 nm τ_{phos} = 9.1 ns $\Phi_{phos} = 3 \times 10^{-3}$%	—	—

Bismuth(V) compounds

To the best of our knowledge, the investigation of the emissive properties of bismuth(V) complexes is confined to two publications. In the first, three bismuthonium salts **85–87** bearing a 1-pyrenyl residue at bismuth(V) display broad, ligand-centred emission at λ_{flu} = 370–500 nm in CH_2Cl_2 at r.t. with quantum yields of up to Φ_{flu} = 4% for **85** (Table 9). Irradiation of these compounds at λ_{exc} < 320 nm results in the liberation of pyrene and the generation of $Bi(Ph\text{-}CH_3)_3$ with photodecomposition quantum yields of Φ_{dec} = 20–22%.[139] A second study focusses on **88**, which phosphoresces in the green region at λ_{phos} = 510 nm with a lifetime of τ_{phos} = 12.7(5) ms in CH_2Cl_2 at 77 K.

Table 9 Summary of the emission properties of bismuth(v) emitters

Ref.	Nr.	Solution, r.t.	Solid, r.t.	Glassy matrix, 77 K
139	**85**	λ_{flu} = 370–500 nm Φ_{flu} = 4%	—	—
139	**86**	λ_{flu} = 370–500 nm Φ_{flu} = 2%	—	—
139	**87**	λ_{flu} = 370–500 nm Φ_{flu} = 2%	—	—
136	**88**	n.o.	n.o.	λ_{phos} = 510 nm τ_{phos} = 12.7(5) ms

Neither fluorescence or phosphorescence emission was found for solutions of **88** at r.t. or in the solid state, possibly due to photodissociation of the halide in the excited states, as was proposed for other Bi-halide compounds.[93] The authors suggest that emission results from a LMCT transition, from lone pairs at the chloride ligands to Bi.[136]

With such a small sample size and differing emphasis of the two studies, it is difficult to draw founded conclusions on the photophysical properties of bismuth(v) compounds. Given the relevance of the bismuth(v) oxidation state in (photo)redox catalysis,[70] additional studies on their photophysical properties seem warranted, however.

Design strategies for emissive Bi complexes

From a theoretical viewpoint, the issue of making emissive Bi complexes seems straightforward: the complex should possess large molar absorption coefficients and undergo fast ISC and no or little radiationless deactivation. From a practical standpoint, the issue is far from simple, however. In this section we focus on the challenges that Bi complexes are associated with and present strategies to overcome these issues.

Enhancing quantum yields through structural rigidity

As described within the section Fundamental principles, radiationless transitions through vibrational relaxation or structural rearrangements are competing processes with emissive transitions. Naturally, the prevention or hampering of radiationless transitions is a common pursuit in the design of luminescent metal complexes, whether they are the transition row, f-block or main group elements.[189] The flexible coordination environment of Bi ions coupled with the weak Bi–E bonds mean that the dissipation of energy through bond cleavage, structural rearrangement within the excited state and vibrational relaxation may become major obstacles. This is especially relevant for phosphors that emit in the red region, where a few vibrational quanta of the ground state may suffice to match with the energy of the excited triplet state (energy gap law).

Indicative of the extent of quenching is the fact that the limited number of Bi complexes that phosphoresce in solution is accompanied by a host of Bi-based coordination polymers, organic–inorganic hybrid materials and inorganic emitters that phosphoresce in the solid state.[58,93,113,119,128,166–168,190–207] For solid state Bi phosphors, several recent reviews emphasize the importance of structural rigidity for the phosphorescence luminescence intensity. This is often achieved through the exclusion of solvent molecules, the incorporation of substituents that support intermolecular interactions and the use of multidentate ligands.[59,128–130,133] For solution emitters, the common pathways to rigidification are the introduction of sterically demanding groups that reduce the degrees of freedom, the use of multidentate ligands, the introduction of groups that can lead to conformational locking through interligand interactions, the shielding of the metal centre to hinder metal–solvent interactions, and the use of structurally inflexible ligands.

To the best of our knowledge, there are no studies that compare the influence of structural rigidity within Bi complexes to their phosphorescence properties directly. However, a large number of authors report on Bi complexes that are non-emissive at r.t. in solution but exhibit phosphorescence at cryogenic temperatures when vibrational relaxation, bond cleavage and other structural rearrangements are hampered. Exemplarily, the triarylbismuth compound **5** (Fig. 3) bearing azaindolophenyl substituents is weakly fluorescent at r.t. in solution, but phosphorescent in the solid state at r.t., in the glassy matrix at 77 K, and as a solid at 77 K.[136] Several other bismuth(III) and bismuth(v) complexes show similar reduced or non-emissive behaviour at r.t., but phosphorescence emission at the same concentrations at cryogenic temperatures.[89,110,122–124,136,141–143,148,151,162–165,178,199]

We note that complexes with Bi–X (X = Cl, Br, I) bonds are especially prone to quenched luminescence at r.t. and it appears reasonable that these compounds are similarly prone to homolytic bond cleavage upon irradiation as the purely inorganic Bi halides.[93–95] Additionally, we note that those few (monomeric) complexes with room-temperature fluorescence or phosphorescence in solution and with quantum yields Φ > 5% are all generally hypervalent and bear structurally rigid ligands such as benzo[h]quinoline, pyrenyl or hyroxyquinolate derivatives.[118,142,160]

Opening new emission pathways through aggregation

Rivard and colleagues have already summarized the properties of several aggregation-induced phosphorescent solid-state emitters of main group elements, including Bi.[59,150] The observance of aggregation-induced emission is not limited to the solid-state, however. For Bi complexes specifically, another possible rigidification pathway arises from Bi's tendency toward hypercoordination. Several studies have shown that the formation of aggregates, usually consisting of dimers formed through bridging heteroatoms between bismuth(III) centres, gives rise to new emission pathways.[89,93,124,140,142,158–160]

Exemplarily, bismuth(III) complexes bearing pyrene ligands **8** (Fig. 3), **27**, **29**, **37** and **38** (Fig. 6) exhibit phosphorescence or fluorescence emission stemming from aggregates,[89,140,142] and the reduction of degrees of freedom is presumed to enhance emission intensity along with the reduction in the energy gap between the excited singlet and triplet states (*cf.* Fig. 13). For

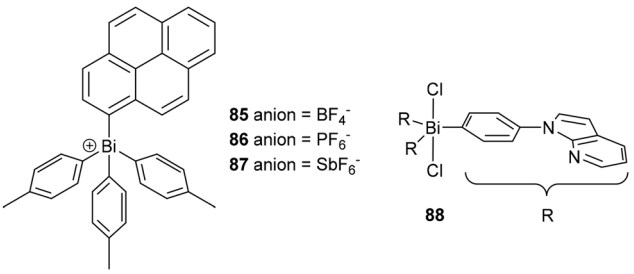

Fig. 12 Molecular structures of bismuth(v) compounds investigated for their emissive properties.

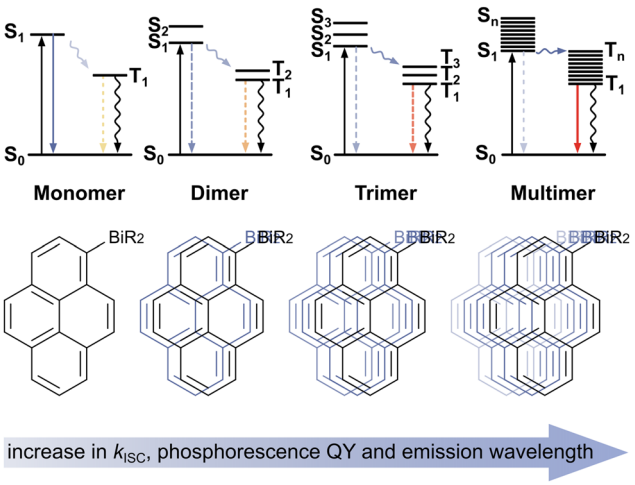

Fig. 13 Schematic representation of the changes in the photophysical pathways of monomers, dimers and aggregates that lead to aggregation-induced emission phenomena.

one of the pyrenyl-modified Bi compounds **38**, quantum chemical calculations show an increased number of distinct electronic states with lower energetic distances between them for the dimer and tetramer.[89] It is assumed that the lowering of excited state energies and smaller energetic differences between the electronic states of the S_n and T_m manifold accelerate ISC and lead to the emergence of phosphorescence.[89,124,142] Other studies by Trogler and colleagues showed that what was long assumed to be fluorescence from Bi tris(8-hydroxyquinolates) **40** and **41** (Fig. 7) in fact stems from dimers, while the monomers fluoresce at significantly higher energies in the UV to blue region.[158–160] In the dimers, the central bismuth(III) ion coordinates to an additional oxygen donor of another complex, giving rise to a 7-fold coordination at Bi.[160] Another recent report by Winter and colleagues focusing on bismuth(III) dihalide complexes with *N*,*C*,*N* pincer ligands **31–36** (Fig. 6) shows an increase of luminescence intensity and the emergence of new emissive features when concentrations are increased, assumed to stem from aggregates.[124] Observations by Schroeder and colleagues on halide-bridged Bi dimers **79–82** (Fig. 10) mirror these observations, showing an increase in luminescence intensity upon aggregation where X = Br or I.[93]

This tendency towards aggregation or dimerization is an interesting opportunity for the emergence of new pathways for emission. If not recognized, however, it may result in the misinterpretation of results as stemming from monomers. This can be rather difficult to elucidate or discount, as the formation of dimers of Bi complexes is not always obvious or expected. Notably, such dimers can form already at very low concentrations of <1 μM.[89] Characteristic to aggregation-induced emission are red-shifted emission spectra, excitation spectra that change noticeably with the detection wavelength, multiexponential emission decay traces, and a marked similarity of the emission feature to that within the solid-state, although the latter may be even further red-shifted.[54,208,209] Aggregation-induced emission can be further probed by investigating the photoluminescence depending on the concentration or by conducting solvent/antisolvent experiments.[54,210]

Enhancing the ISC rate through CT transitions

For the transition d-block elements it has been shown that electronic excitation with a distinct CT character is beneficial for the observation of fast ISC and phosphorescence with high quantum yields.[47,48,63,189] Based on the findings for the transition row elements, it has been suggested that metal contributions to low-energy transitions are crucial for the emergence of the r.t. phosphorescence of Bi complexes.[118]

Several examples of phosphorescent Bi complexes with MLCT, LL′CT, LMXCT and XMLCT characters of their lowest-energy transition are supportive of this argument. The complex with the highest phosphorescence quantum yield at r.t. to date is **51** (Fig. 7 or Fig. 14) with a reported QY of Φ_{phos} = 10(3)%. **51** exhibits an MLCT type transition at *ca.* 500 nm as its lowest-energy transition.[118] The only two publications that report on the emissive properties of bismuth(I) complexes also note an MLCT transition as the lowest-energy transition. These closely related Dostál-type bismuth(I) complexes **83** and **84** (Fig. 11) emit in the NIR region of the spectrum at r.t. in solution, albeit with very low quantum yields of Φ_{phos} = 0.005% and 0.003%, respectively.[110,188] For one of the two complexes, transient absorption spectroscopy (TAS) studies indicate that ISC takes place within τ = 2.2 ps.[188] Other bismuth(III) com-

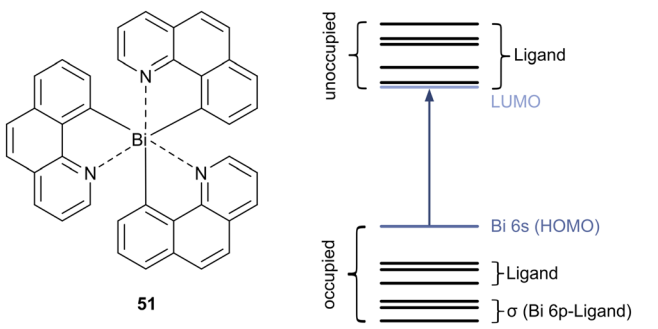

Fig. 14 Schematic representation of an MO diagram of **51**.

plexes **15–18** (Fig. 5) with LL′CT transitions as their lowest-energy electronic excitation exhibit r.t. phosphorescence despite little Bi contribution to either of the DFT-calculated occupied or unoccupied MOs.[125] The lowest-energy bands of several bismuth(III) halide complexes bearing pyrrolide or dipyrrolide ligands **68–78** (Fig. 10) were computed to be of the LMXCT character with electron density shifting from the electron-rich ligands to MOs with a distinct Bi-halide antibonding character.[122,123,178] These complexes are non-emissive at r.t. but phosphorescent in glassy matrices with quantum yields of up to Φ_{phos} = 50.8%.[123] Other bismuth(III) halide complexes **31–36** (Fig. 6) with *N*,*C*,*N* pincer ligands and LMXCT type transitions as their lowest-energy excitation exhibit weak fluorescence emission in solution at r.t., but stronger phosphorescence emission of up to Φ_{phos} = 47% at cryogenic temperatures.[124] LMXCT transitions were reported for **88** with bismuth(V) (Fig. 12), which is non-emissive at r.t. but phosphoresces at 77 K.[136] Finally, a complex in which the lowest-energy transitions were determined to be of a partial MXLCT nature is **39** (Fig. 6) which is non-emissive at r.t. but phosphorescent at λ_{phos} = 500 nm at 77 K.[110]

Further supportive of the CT argument is the fact that those complexes wherein predominantly π–π* transitions are observed are generally not phosphorescent at r.t. Instead, these compounds are either non-emissive or fluorescent at r.t. in solution with low quantum yields compared to the corresponding pure ligands or chromophores.[136–138,140–143,146–148,159,160,172–174,176,177]
Interestingly, a few such emitters were shown to produce singlet oxygen, indicating that a relatively long-lived dark triplet state with lifetime at least in the ns regime is quenched by triplet oxygen.[146,147]

Contradictory to the CT argument are two reports on room-temperature phosphorescent Bi complexes in which all relevant electronic transitions were calculated to be of a π–π* character. Both the so-called dithienobismoles **19–22** (Fig. 5) and metal–organic Bi compounds with boron acceptor units **11** and **12** (Fig. 4) were shown to be dually emissive at r.t. in solution.[126,127] Here, the population of the excited triplet state is assumed to rely on small energy differences between the excited singlet and triplet states and large SOCCs between these states. In both instances the authors nevertheless emphasize the importance of the remote heavy atom effect of Bi.

Enhancing stability through coordinating ligands and sterically demanding substituents

The long Bi–C bonds of ≈2.27 Å[74] and the low bond dissociation energy of Bi–C bonds of 46 kcal mol^{-1},[80] which arise from the poor orbital overlap between the C-atoms and Bi's large, diffuse and polarizable AOs, may render them labile. A host of publications report homolytic cleavage of Bi–C bonds in organometallic Bi complexes,[81–86] and unsurprisingly, homolytic bond cleavage of Bi–O[87,88] Bi–S,[89] Bi–N[90,91] or Bi–Br[92] and Bi–I[93–95] bonds through either light or thermal energy has been reported as well. Moreover, Bi–halide bonds are sensitive towards moisture as noted by Greenwood and Earnshaw.[211]

The general sensitivity of Bi compounds is reflected in several reports on Bi emitters. Exemplarily, **51** (Fig. 7 and 14) decomposes within a few seconds upon irradiation at $\lambda_{exc} \leq$ 390 nm in solution,[118] and complexes **23–26** in which Bi is incorporated into a Rhodamine-type scaffold (Fig. 5) are reported to degrade by *ca.* 15% over the course of 60 min under irradiation with red light at λ_{exc} = 625 nm.[146] Irradiation of Bi complexes with arylthiolate ligands **27–30** (Fig. 6) at r.t. in solution leads to the isolation of the corresponding disulfide ArS–SAr.[89] Rivard and colleagues note the decomposition of bismole derivatives under ambient conditions[151] while Ohshita *et al.* note moisture sensitivity for thienylbismuth compounds **10–12** (Fig. 4).[126]

The most common strategy for enhancing the stability of Bi complexes is to employ multidentate anionic ligands,[96] usually with nitrogen or oxygen donors. Exemplarily, the incorporation of additional oxygen donors on the ligands of Bi complexes **66** and **67** (Fig. 9) with dipyrrin ligands is reported to lead to "a significantly increased stability in solution" compared to the unsubstituted congeners reported previously by the same authors.[172,177] The incorporation of ligands with donating capabilities was also pursued for several Bi complexes **31–37** and **39** with tridentate diamine or diimine *N*,*C*,*N*-pincer ligands (Fig. 6), which were found to be stable towards light upon irradiation at λ_{exc} = 365 nm over several minutes.[110,124,142]

Another strategy for increasing the stability of Bi complexes is to add steric bulk around the Bi centre. Exemplarily, the addition of sterically demanding groups such as xylyl (Xyl), ^{t}butyl (^{t}Bu) or others at the ligands of Dostál-type bismuth(I) complexes such as **83** and **84** (Fig. 11) shields the reactive bismuth(I) centre and prevents these complexes from dimerizing.[104] Similarly, the use of mesityl- (Mes-) or ^{t}Bu-substituted pyridine dipyrrolide ligands in complexes **68** and **72** (Fig. 10) enhances their stability compared to the equivalent –CH_3 substituted compounds **69–71**.[122] Ohshita and colleagues observed rapid decomposition in dilute solutions and even in the solid state for dithienobismoles **20** and **21** (Fig. 5) lacking sterically shielding groups, while those with methyl substituents and benzo-annulated rings **19** and **22** (Fig. 5) were stable.[127]

Conclusions

With this literature overview, we have presented several strategies for the generation of phosphorescent Bi compounds. Most studies have focussed on bismuth(III) phosphors and only two reports each on bismuth(I) and bismuth(V) emitters are presently available.

On the one hand, the large SOC constant of Bi and its good availability, affordable pricing and low toxicity make it an attractive element for the generation of phosphorescent materials. On the other hand, Bi compounds are accompanied by a number of challenges depending on their oxidation state: (i) weak Bi–E bonds, which may lead to light-, moisture- or

temperature-sensitive compounds; (ii) generally long Bi–E bonds can lead to reduced structural rigidity that enables the non-radiative dissipation of energy through structural reorganisation in the photoexcited state; (iii) the capability to engage in hypervalent bonding through 3-centre-4-electron bonds leading to energetically low-lying unoccupied Bi-ligand antibonding orbitals whose population may quench luminescence through homolytic bond cleavage or large-amplitude structural distortions in the excited state; (iv) a generally high reactivity for bismuth(I) compounds; (v) low hybridization of the 6s and 6p atomic orbitals for bismuth(III) compounds, giving rise to a largely inert s-type lone pair at Bi that does not interact with ligand orbitals and prevents energetically low-lying electronic transitions with a (partial) metal character. Addressing these challenges is not trivial and consequently, only six instances of r.t. phosphorescence in solution have been reported for monomeric Bi complexes thus far.[110,118,125–127,188] Instead, most Bi complexes investigated for their solution luminescent behaviour are non-emissive or weakly fluorescent at r.t., although investigations on these same complexes within the solid state or in frozen solutions at 77 K reveal phosphorescence emission. The limited number of phosphorescent solution emitters is accompanied by an abundance of solid-state emissive bismuth compounds and a few studies show that, despite the lack of an emissive triplet state at r.t., bismuth complexes are nevertheless able to generate singlet oxygen, which is promising for future applications and shows that triplet states are indeed being populated.

Several strategies have emerged as promising for the generation of phosphorescent Bi materials:

(1) The use of multidentate, rigid ligands hampers the non-radiative dissipation of energy to the environment.

(2) The use of multidentate ligands may alleviate the issues of light sensitivity that many bismuth(III) and bismuth(V) compounds face.

(3) The propensity of especially bismuth(III) complexes to hypercoordination opens pathways toward aggregation-induced phosphorescence. For this, the use of ligands with heteroatoms capable of bridging Bi-monomers or the incorporation of ligands with π-stacking capabilities have been successful in the literature.

(4) Sterically demanding or additional donor substituents capable of coordinating to the Bi ion enhance the stability of Bi phosphors by shielding the metal ions.

(5) The use of ligands with neutral donors capable of coordinating to the Bi ion provides MOs that can interact with Bi to endow energetically low-lying electronic transitions with a (partial) metal character, which enhances ISC and phosphorescence rate constants. MLCT transitions appear especially promising as seen by the room-temperature NIR emission of bismuthinidenes.

Conflicts of interest

There are no conflicts to declare.

Data availability

No primary research results, software or code have been included and no new data were generated or analysed as part of this review.

References

1 F. Strieth-Kalthoff and F. Glorius, Triplet Energy Transfer Photocatalysis: Unlocking the Next Level, *Chem*, 2020, **6**, 1888–1903.
2 S. Dutta, J. E. Erchinger, F. Strieth-Kalthoff, R. Kleinmans and F. Glorius, Energy transfer photocatalysis: exciting modes of reactivity, *Chem. Soc. Rev.*, 2024, **53**, 1068–1089.
3 L. G. Franca, D. G. Bossanyi, J. Clark and P. L. dos Santos, Exploring the Versatile Uses of Triplet States: Working Principles, Limitations, and Recent Progress in Phosphorescence, TADF, and TTA, *ACS Appl. Opt. Mater.*, 2024, **2**, 2476–2500.
4 K. Sharma, V. Sharma and S. S. Sharma, Dye-Sensitized Solar Cells: Fundamentals and Current Status, *Nanoscale Res. Lett.*, 2018, **13**, 381.
5 C. Bizzarri, E. Spuling, D. M. Knoll, D. Volz and S. Bräse, Sustainable metal complexes for organic light-emitting diodes (OLEDs), *Coord. Chem. Rev.*, 2018, **373**, 49–82.
6 Y. Chi and P.-T. Chou, Transition-metal phosphors with cyclometalating ligands: fundamentals and applications, *Chem. Soc. Rev.*, 2010, **39**, 638–655.
7 X. Li, Y. Xie and Z. Li, Diversity of Luminescent Metal Complexes in OLEDs: Beyond Traditional Precious Metals, *Chem. – Asian J.*, 2021, **16**, 2817–2829.
8 A. J. Carrod, V. Gray and K. Börjesson, Recent advances in triplet–triplet annihilation upconversion and singlet fission, towards solar energy applications, *Energy Environ. Sci.*, 2022, **15**, 4982–5016.
9 T. Huang, Q. Yu, S. Liu, W. Huang and Q. Zhao, Phosphorescent iridium(III) complexes: a versatile tool for biosensing and photodynamic therapy, *Dalton Trans.*, 2018, **47**, 7628–7633.
10 S. Monro, K. L. Colón, H. Yin, J. Roque, P. Konda, S. Gujar, R. P. Thummel, L. Lilge, C. G. Cameron and S. A. McFarland, Transition Metal Complexes and Photodynamic Therapy from a Tumor-Centered Approach: Challenges, Opportunities, and Highlights from the Development of TLD1433, *Chem. Rev.*, 2019, **119**, 797–828.
11 J. Herberger and R. F. Winter, Platinum emitters with dye-based σ-aryl ligands, *Coord. Chem. Rev.*, 2019, **400**, 213048.
12 D. Ruggeri, M. Hoch, D. Spataro, L. Marchiò, S. Protti, D. Cauzzi, M. Tegoni, M. Lanzi and G. Maestri, Tuning the Efficiency of Iridium(III) Complexes for Energy Transfer (EnT) Catalysis through Ligand Design, *Chem. – Eur. J.*, 2025, **31**, e202403309.
13 B. Pashaei, H. Shahroosvand, M. Graetzel and M. K. Nazeeruddin, Influence of Ancillary Ligands in Dye-Sensitized Solar Cells, *Chem. Rev.*, 2016, **116**, 9485–9564.

14 P. I. Djurovich, D. Murphy, M. E. Thompson, B. Hernandez, R. Gao, P. L. Hunt and M. Selke, Cyclometalated iridium and platinum complexes as singlet oxygen photosensitizers: quantum yields, quenching rates and correlation with electronic structures, *Dalton Trans.*, 2007, 3763–3770, DOI: 10.1039/B704595F.
15 D. Ma, T. Tsuboi, Y. Qiu and L. Duan, Recent Progress in Ionic Iridium(III) Complexes for Organic Electronic Devices, *Adv. Mater.*, 2017, **29**, 1603253.
16 H. Yersin, A. F. Rausch, R. Czerwieniec, T. Hofbeck and T. Fischer, The triplet state of organo-transition metal compounds. Triplet harvesting and singlet harvesting for efficient OLEDs, *Coord. Chem. Rev.*, 2011, **255**, 2622–2652.
17 T. Hofbeck and H. Yersin, The Triplet State of fac-Ir(ppy)$_3$, *Inorg. Chem.*, 2010, **49**, 9290–9299.
18 W. Holzer, A. Penzkofer and T. Tsuboi, Absorption and emission spectroscopic characterization of Ir(ppy)$_3$, *Chem. Phys.*, 2005, **308**, 93–102.
19 S.-R. Kang, Z.-Q. Zhou, C.-F. Xiong, B. Liu, J. E. McGrady, M. Obies, C. Liu, P. He and X.-Y. Yi, Structural, spectroscopic and electronic properties of a family of face-shared bi-octahedral $Ru_2^{5+/6+}$ complexes with a bridging 2,5-di(2-pyridyl)pyrrolide ligand, *Dalton Trans.*, 2020, **49**, 7053–7059.
20 A. S. Polo, M. K. Itokazu and N. Y. M. Iha, Metal complex sensitizers in dye-sensitized solar cells, *Coord. Chem. Rev.*, 2004, **248**, 1343–1361.
21 P. Irmler, F. S. Gogesch, A. Mang, M. Bodensteiner, C. B. Larsen, O. S. Wenger and R. F. Winter, Directing energy transfer in Pt(bodipy)(mercaptopyrene) dyads, *Dalton Trans.*, 2019, **48**, 11690–11705.
22 M. Montalti, A. Credi, L. Prodi and M. T. Gandolfi, *Handbook of Photochemistry*, CRC Press, Boca Raton, 3 edn, 2006.
23 S. Fraga, J. Karwowski and K. M. S. Saxena, *Handbook of Atomic Data*, Elsevier Scientific Publishing Company (Amsterdam, Oxford, New York), 1976.
24 Y. Sano, H. Satoh, M. Chiba, M. Okamoto, K. Serizawa, H. Nakashima and K. Omae, Oral Toxicity of Bismuth in Rat: Single and 28-Day Repeated Administration Studies, *J. Occup. Health*, 2005, **47**, 293–298.
25 J. D. Rosário, F. H. Moreira, L. H. Rosa, W. Guerra and P. P. Silva-Caldeira, Biological Activities of Bismuth Compounds: An Overview of the New Findings and the Old Challenges Not Yet Overcome, *Molecules*, 2023, **28**, 5921.
26 D. M. Griffith, H. Li, M. V. Werrett, P. C. Andrews and H. Sun, Medicinal chemistry and biomedical applications of bismuth-based compounds and nanoparticles, *Chem. Soc. Rev.*, 2021, **50**, 12037–12069.
27 Â. Gonçalves, M. Matias, J. A. R. Salvador and S. Silvestre, Bioactive Bismuth Compounds: Is Their Toxicity a Barrier to Therapeutic Use?, *Int. J. Mol. Sci.*, 2024, **25**, 1600.
28 A. Slikkerveer, R. B. Helmich, P. M. Edelbroek, G. B. van der Voet and F. A. de Wolff, Analysis of bismuth in serum and blood by electrothermal atomic absorption spectrometry using platinum as matrix modifier, *Clin. Chim. Acta*, 1991, **201**, 17–25.
29 F. de Wolff and A. Slikkerveer, *Toxicology of Metals, Volume I*, CRC Press (Boca Raton), 1996, pp. 439–454..
30 V. Supino-Viterbo, C. Sicard, M. Risvegliato, G. Rancurel and A. Buge, Toxic encephalopathy due to ingestion of bismuth salts: clinical and EEG studies of 45 patients, *J. Neurol., Neurosurg. Psychiatry.*, 1977, **40**, 748.
31 İ. İşlek, S. Uysal, F. Gök, R. Dündaröz and Ş. Küçüködük, Reversible nephrotoxicity after overdose of colloidal bismuth subcitrate, *Pediatr. Nephrol.*, 2001, **16**, 510–514.
32 B. Bialek, R. A. Diaz-Bone, D. Pieper, M. Hollmann and R. Hensel, Toxicity of Methylated Bismuth Compounds Produced by Intestinal Microorganisms to Bacteroides thetaiotaomicron, a Member of the Physiological Intestinal Microbiota, *J. Toxicol.*, 2011, 608349.
33 E. Dopp, U. von Recklinghausen, J. Hippler, R. A. Diaz-Bone, J. Richard, U. Zimmermann, A. W. Rettenmeier and A. V. Hirner, Toxicity of Volatile Methylated Species of Bismuth, Arsenic, Tin, and Mercury in Mammalian Cells In Vitro, *J. Toxicol.*, 2011, **2011**, 503576.
34 Y. Cui, L. Yang, X. Wu, J. Deng, X. Zhang and J. Zhang, Recent progress of lead-free bismuth-based perovskite materials for solar cell applications, *J. Mater. Chem. C*, 2022, **10**, 16629–16656.
35 Z. Jin, Z. Zhang, J. Xiu, H. Song, T. Gatti and Z. He, A critical review on bismuth and antimony halide based perovskites and their derivatives for photovoltaic applications: recent advances and challenges, *J. Mater. Chem.*, 2020, **8**, 16166–16188.
36 P. Boutinaud, Luminescence–structure relationships in solids doped with Bi^{3+}, *Phys. Chem. Chem. Phys.*, 2023, **25**, 11027–11054.
37 Y. Tang, M. Deng, M. Wang, X. Liu, Z. Zhou, J. Wang and Q. Liu, Bismuth-Activated Persistent Phosphors, *Adv. Opt. Mater.*, 2023, **11**, 2201827.
38 R. Ma, X. Gong, C. Deng and W. Huang, Bismuth-activated luminescence reversible modification of photochromic for multimodal anti-counterfeiting and optical storage application, *J. Alloys Compd.*, 2025, **1022**, 179812.
39 X. Zhang, J.-X. Hao, M.-L. Cai, B. Zhang, X.-M. Zhen and Y. Wu, Spatial & Temporal Dual-Resolved Anti-Counterfeiting Applications in a Long Afterglow System Based on Bismuth Halides, *Inorg. Chem.*, 2025, **64**, 8238–8249.
40 D. Gao, C. Du, Y. Wang, W. Xu, W. Gao, Q. Pang and Y. Wang, Controllable persistent luminescence in bismuth activated memory phosphors by trap management for artificial intelligence anti-counterfeiting, *J. Mater. Chem. C*, 2024, **12**, 19487–19497.
41 M. Peng, Q. Zhao, J. Qiu and L. Wondraczek, Generation of Emission Centers for Broadband NIR Luminescence in Bismuthate Glass by Femtosecond Laser Irradiation, *J. Am. Ceram. Soc.*, 2009, **92**, 542–544.
42 K. Udaya Kumar, P. Babu, C. Basavapoornima, R. Praveena, D. Shobha Rani and C. K. Jayasankar,

Spectroscopic properties of Nd^{3+}-doped boro-bismuth glasses for laser applications, *Phys. B: Condens. Matter*, 2022, **646**, 414327.

43 F. Tan, D. Chen, S. Ge, C. Jiang, Y. Zhang, Z. Zhang, S. Cui and Z. Leng, Luminescence properties and application of near-infrared Er^{3+}-doped bismuth germanate laser glass, *Opt. Commun.*, 2025, **591**, 132167.

44 J. W. Verhoeven, Glossary of terms used in photochemistry (IUPAC Recommendations 1996), *Pure Appl. Chem.*, 1996, **68**, 2223–2286.

45 K. Ruud, B. Schimmelpfennig and H. Ågren, Internal and external heavy-atom effects on phosphorescence radiative lifetimes calculated using a mean-field spin–orbit Hamiltonian, *Chem. Phys. Lett.*, 1999, **310**, 215–221.

46 M. Mońka, I. E. Serdiuk, K. Kozakiewicz, E. Hoffman, J. Szumilas, A. Kubicki, S. Y. Park and P. Bojarski, Understanding the internal heavy-atom effect on thermally activated delayed fluorescence: application of Arrhenius and Marcus theories for spin–orbit coupling analysis, *J. Mater. Chem. C*, 2022, **10**, 7925–7934.

47 G. Baryshnikov, B. Minaev and H. Ågren, Theory and Calculation of the Phosphorescence Phenomenon, *Chem. Rev.*, 2017, **117**, 6500–6537.

48 B. Minaev, G. Baryshnikov and H. Agren, Principles of phosphorescent organic light emitting devices, *Phys. Chem. Chem. Phys.*, 2014, **16**, 1719–1758.

49 T. J. Penfold, E. Gindensperger, C. Daniel and C. M. Marian, Spin-Vibronic Mechanism for Intersystem Crossing, *Chem. Rev.*, 2018, **118**, 6975–7025.

50 C. M. Marian, Spin–orbit coupling and intersystem crossing in molecules, *Wiley Interdiscip. Rev.:Comput. Mol. Sci.*, 2012, **2**, 187–203.

51 N. J. Turro, V. Ramamurthy and J. C. Scaiano, *Modern Molecular Photochemistry of Organic Molecules*, University Science Books, Sausalito, California, 2010.

52 C. M. Marian, Understanding and Controlling Intersystem Crossing in Molecules, *Annu. Rev. Phys. Chem.*, 2021, **72**, 617–640.

53 R. Englman and J. Jortner, The energy gap law for radiationless transitions in large molecules, *Mol. Phys.*, 1970, **18**, 145–164.

54 J. Mei, N. L. C. Leung, R. T. K. Kwok, J. W. Y. Lam and B. Z. Tang, Aggregation-Induced Emission: Together We Shine, United We Soar!, *Chem. Rev.*, 2015, **115**, 11718–11940.

55 Y. Zhang, T. S. Lee, J. L. Petersen and C. Milsmann, A Zirconium Photosensitizer with a Long-Lived Excited State: Mechanistic Insight into Photoinduced Single-Electron Transfer, *J. Am. Chem. Soc.*, 2018, **140**, 5934–5947.

56 H. Uoyama, K. Goushi, K. Shizu, H. Nomura and C. Adachi, Highly efficient organic light-emitting diodes from delayed fluorescence, *Nature*, 2012, **492**, 234–238.

57 L. Yang, X. Wang, G. Zhang, X. Chen, G. Zhang and J. Jiang, Aggregation-induced intersystem crossing: a novel strategy for efficient molecular phosphorescence, *Nanoscale*, 2016, **8**, 17422–17426.

58 S. M. Parke, E. Hupf, G. K. Matharu, I. Aguiar, L. Xu, H. Yu, M. P. Boone, G. L. C. Souza, R. McDonald, M. J. Ferguson, G. He, A. Brown and E. Rivard, Aerobic Solid State Red Phosphorescence from Benzobismole Monomers and Patternable Self-Assembled Block Copolymers, *Angew. Chem., Int. Ed.*, 2018, **57**, 14841–14846.

59 S. M. Parke and E. Rivard, Aggregation Induced Phosphorescence in the Main Group, *Isr. J. Chem.*, 2018, **58**, 915–926.

60 E. M. Kober, B. P. Sullivan and T. J. Meyer, Solvent dependence of metal-to-ligand charge-transfer transitions. Evidence for initial electron localization in MLCT excited states of 2,2′-bipyridine complexes of ruthenium(II) and osmium(II), *Inorg. Chem.*, 1984, **23**, 2098–2104.

61 N. S. Hush and J. R. Reimers, Solvent Effects on the Electronic Spectra of Transition Metal Complexes, *Chem. Rev.*, 2000, **100**, 775–786.

62 N. J. Turro, *Modern Molecular Photochemistry*, The Banjamin/Cummings Publishign Co., Inc., Menlo Park, California, 1978.

63 P.-T. Chou, Y. Chi, M.-W. Chung and C.-C. Lin, Harvesting luminescence via harnessing the photophysical properties of transition metal complexes, *Coord. Chem. Rev.*, 2011, **255**, 2653–2665.

64 E. M. Kober, J. V. Caspar, R. S. Lumpkin and T. J. Meyer, Application of the energy gap law to excited-state decay of osmium(II)-polypyridine complexes: calculation of relative nonradiative decay rates from emission spectral profiles, *J. Phys. Chem.*, 1986, **90**, 3722–3734.

65 V. L. Ermolaev and E. B. Sveshnikova, The application of luminescence-kinetic methods in the study of the formation of lanthanide ion complexes in solution, *Russ. Chem. Rev.*, 1994, **63**, 905.

66 J. B. Birks, D. J. Dyson and I. H. Munro, 'Excimer' fluorescence II. Lifetime studies of pyrene solutions, *Proc. – R. Soc. Edinburgh, Sect. A*, 1963, **275**, 575–588.

67 J. B. Birks, *Photophysics of aromatic molecules*, Wiley, London, 1970.

68 Y. Hong, J. W. Y. Lam and B. Z. Tang, Aggregation-induced emission, *Chem. Soc. Rev.*, 2011, **40**, 5361–5388.

69 L. D. Freedman and G. O. Doak, Preparation, reactions, and physical properties of organobismuth compounds, *Chem. Rev.*, 1982, **82**, 15–57.

70 M. Mato and J. Cornella, Bismuth in Radical Chemistry and Catalysis, *Angew. Chem., Int. Ed.*, 2024, **63**, e202315046.

71 H. Suzuki, N. Komatsu, T. Ogawa, T. Murafuji, T. Ikegami and Y. Matano, *Organobismuth Chemistry*, Elsevier Science B. V., Amsterdam, the Netherlands, 1 edn., 2001.

72 A. Gagnon, J. Dansereau and A. Le Roch, Organobismuth Reagents: Synthesis, Properties and Applications in Organic Synthesis, *Synthesis*, 2017, 1707–1745.

73 A. Das, U. Das and A. K. Das, Relativistic effects on the chemical bonding properties of the heavier elements and their compounds, *Coord. Chem. Rev.*, 2023, **479**, 215000.

74 C. Silvestru, H. J. Breunig and H. Althaus, Structural Chemistry of Bismuth Compounds. I. Organobismuth Derivatives, *Chem. Rev.*, 1999, **99**, 3277–3328.
75 R. D. Rogers, A. H. Bond, S. Aguinaga and A. Reyes, Complexation chemistry of bismuth(III) halides with crown ethers and polyethylene glycols. Structural manifestations of a stereochemically active lone pair, *J. Am. Chem. Soc.*, 1992, **114**, 2967–2977.
76 C. Harriswangler, F. Lucio-Martínez, A. Rodríguez-Rodríguez, D. Esteban-Gómez and C. Platas-Iglesias, Unravelling the 6sp ← 6s absorption spectra of Bi(III) complexes, *Dalton Trans.*, 2024, **53**, 2275–2285.
77 C. Lichtenberg, Molecular bismuth(III) monocations: structure, bonding, reactivity, and catalysis, *Chem. Commun.*, 2021, **57**, 4483–4495.
78 D. L. G. Symes and J. D. Masuda, Recent advances in heavier group 15 (P, As, Sb, Bi) radical chemistry – frameworks, small molecule reactivity, and catalysis, *Dalton Trans.*, 2025, **54**, 5234–5249.
79 S. Ishida, F. Hirakawa and T. Iwamoto, A Series of Two-Coordinate Group-15 Element (P, As, Sb, Bi) Centered Radicals Having Bulky Alkyl Groups, *Bull. Chem. Soc. Jpn.*, 2018, **91**, 1168–1175.
80 W. V. Steele, The standard enthalpies of formation of the triphenyl compounds of the Group V elements 2. Triphenylbismuth and the Ph–Bi mean bond-dissociation energy, *J. Chem. Thermodyn.*, 1979, **11**, 187–192.
81 N. D. Chiappini, E. P. Geunes, E. T. Bodak and R. R. Knowles, Organobismuth Compounds as Aryl Radical Precursors via Light-Driven Single-Electron Transfer, *ACS Catal.*, 2024, **14**, 2664–2670.
82 D. H. Hey, D. A. Shingleton and G. H. Williams, 1075. Homolytic aromatic substitution. Part XXIX. The photolysis of triphenylbismuth in aromatic solvents, *J. Chem. Soc.*, 1963, 5612–5619, DOI: 10.1039/JR9630005612.
83 M. Nakajima, S. Nagasawa, K. Matsumoto, T. Kuribara, A. Muranaka, M. Uchiyama and T. Nemoto, A Direct $S_0 \rightarrow T_n$ Transition in the Photoreaction of Heavy-Atom-Containing Molecules, *Angew. Chem., Int. Ed.*, 2020, **59**, 6847–6852.
84 K. Oberdorf, A. Hanft, X. Xie, F. M. Bickelhaupt, J. Poater and C. Lichtenberg, Insertion of CO_2 and CS_2 into Bi–N bonds enables catalyzed CH-activation and light-induced bismuthinidene transfer, *Chem. Sci.*, 2023, **14**, 5214–5219.
85 S. Yamago, E. Kayahara, M. Kotani, B. Ray, Y. Kwak, A. Goto and T. Fukuda, Highly Controlled Living Radical Polymerization through Dual Activation of Organobismuthines, *Angew. Chem., Int. Ed.*, 2007, **46**, 1304–1306.
86 J. Lorberth, W. Massa, S. Wocadlo, I. Sarraje, S. H. Shin and X. W. Li, Synthesis and crystal structure of E.O. Fischer's "red crystalline modification of tris-cyclopentadienylbismuth, $(1h\text{-}C_5H_5)_3Bi$", *J. Organomet. Chem.*, 1995, **485**, 149–152.
87 T. A. Hanna, A. L. Rieger, P. H. Rieger and X. Wang, Evidence for an Unstable Bi(II) Radical from Bi–O Bond Homolysis. Implications in the Rate-Determining Step of the SOHIO Process, *Inorg. Chem.*, 2002, **41**, 3590–3592.
88 X. Kou, X. Wang, D. Mendoza-Espinosa, L. N. Zakharov, A. L. Rheingold, W. H. Watson, K. A. Brien, L. K. Jayarathna and T. A. Hanna, Bismuth Aryloxides, *Inorg. Chem.*, 2009, **48**, 11002–11016.
89 M. Geppert, K. Jellinek, M. Linseis, M. Bodensteiner, J. Geppert, M. Unterlass and R. F. Winter, Dual Fluorescence and Phosphorescence Emissions from Dye-Modified (NCN)-Bismuth Pincer Thiolate Complexes, *Inorg. Chem.*, 2024, **63**, 14876–14888.
90 X. Yang, E. J. Reijerse, K. Bhattacharyya, M. Leutzsch, M. Kochius, N. Nöthling, J. Busch, A. Schnegg, A. A. Auer and J. Cornella, Radical Activation of N–H and O–H Bonds at Bismuth(II), *J. Am. Chem. Soc.*, 2022, **144**, 16535–16544.
91 W. Clegg, N. A. Compton, R. J. Errington, G. A. Fisher, M. E. Green, D. C. R. Hockless and N. C. Norman, X-ray crystal structure of bismuth dimethylamide, *Inorg. Chem.*, 1991, **30**, 4680–4682.
92 K. Oldenburg and A. Vogler, Electronic Spectra and Photochemistry of Tin(II), Lead(II), Antimony(III), and Bismuth(III) Bromide Complexes in Solution, *Z. Naturforsch., B*, 1993, **48**, 1519–1523.
93 H. Bhatia, J. Guo, C. N. Savory, M. Rush, D. I. James, A. Dey, C. Chen, D.-K. Bučar, T. M. Clarke, D. O. Scanlon, R. G. Palgrave and B. C. Schroeder, Exploring Bismuth Coordination Complexes as Visible-Light Absorbers: Synthesis, Characterization, and Photophysical Properties, *Inorg. Chem.*, 2024, **63**, 416–430.
94 E. H. Choi, D.-S. Ahn, S. Park, C. Kim, C. W. Ahn, S. Kim, M. Choi, C. Yang, T. W. Kim, H. Ki, J. Choi, M. N. Pedersen, M. Wulff, J. Kim and H. Ihee, Structural Dynamics of Bismuth Triiodide in Solution Triggered by Photoinduced Ligand-to-Metal Charge Transfer, *J. Phys. Chem. Lett.*, 2019, **10**, 1279–1285.
95 O. Horváth and I. Mikó, Spectra, equilibrium and photoredox chemistry of iodobismuthate(III) complexes in acetonitrile, *Inorg. Chim. Acta*, 2000, **304**, 210–218.
96 J. Hyvl, Hypervalent organobismuth complexes: pathways toward improved reactivity, catalysis, and applications, *Dalton Trans.*, 2023, **52**, 12597–12603.
97 M. K. Pandey, D. Mondal, B. S. Kote and M. S. Balakrishna, Synthesis and Photophysical Properties of Heavier Pnictogen Complexes, *ChemPlusChem*, 2023, **88**, e202200460.
98 C. I. Raț, C. Silvestru and H. J. Breunig, Hypervalent organoantimony and -bismuth compounds with pendant arm ligands, *Coord. Chem. Rev.*, 2013, **257**, 818–879.
99 X. Chen, Y. Yamamoto and K.-Y. Akiba, Hypervalent tetracoordinate organobismuth compounds (10-Bi-4), *Heteroat. Chem.*, 1995, **6**, 293–303.
100 M. L. H. Green and G. Parkin, The classification and representation of main group element compounds that feature three-center four-electron interactions, *Dalton Trans.*, 2016, **45**, 18784–18795.

101 Y. Pang, N. Nöthling, M. Leutzsch, L. Kang, E. Bill, M. van Gastel, E. Reijerse, R. Goddard, L. Wagner, D. SantaLucia, S. DeBeer, F. Neese and J. Cornella, Synthesis and isolation of a triplet bismuthinidene with a quenched magnetic response, *Science*, 2023, **380**, 1043–1048.

102 Y. Schulte, T. Freese, C. Wölper, J. Schulte, G. Haberhauer and S. Schulz, Synthesis and Reactivity of a Mono-Coordinated Triplet Bismuthinidene, *Angew. Chem., Int. Ed.*, 2025, **64**, e202508250.

103 M. Wu, W. Chen, D. Wang, Y. Chen, S. Ye and G. Tan, Triplet bismuthinidenes featuring unprecedented giant and positive zero field splittings, *Natl. Sci. Rev.*, 2023, **10**, nwad169.

104 P. Šimon, F. de Proft, R. Jambor, A. Růžička and L. Dostál, Monomeric Organoantimony(I) and Organobismuth(I) Compounds Stabilized by an NCN Chelating Ligand: Syntheses and Structures, *Angew. Chem., Int. Ed.*, 2010, **49**, 5468–5471.

105 L. Dostál, Quest for stable or masked pnictinidenes: Emerging and exciting class of group 15 compounds, *Coord. Chem. Rev.*, 2017, **353**, 142–158.

106 L. Dostál, R. Jambor, M. Aman and M. Hejda, (N),C, N-Coordinated Heavier Group 13–15 Compounds: Synthesis, Structure and Applications, *ChemPlusChem*, 2020, **85**, 2320–2340.

107 I. Vránová, M. Alonso, R. Lo, R. Sedlák, R. Jambor, A. Růžička, F. D. Proft, P. Hobza and L. Dostál, From Dibismuthenes to Three- and Two-Coordinated Bismuthinidenes by Fine Ligand Tuning: Evidence for Aromatic BiC_3N Rings through a Combined Experimental and Theoretical Study, *Chem. – Eur. J.*, 2015, **21**, 16917–16928.

108 M. M. Siddiqui, S. K. Sarkar, M. Nazish, M. Morganti, C. Köhler, J. Cai, L. Zhao, R. Herbst-Irmer, D. Stalke, G. Frenking and H. W. Roesky, Donor-Stabilized Antimony(I) and Bismuth(I) Ions: Heavier Valence Isoelectronic Analogues of Carbones, *J. Am. Chem. Soc.*, 2021, **143**, 1301–1306.

109 J. Xu, S. Pan, S. Yao, C. Lorent, C. Teutloff, Z. Zhang, J. Fan, A. Molino, K. B. Krause, J. Schmidt, R. Bittl, C. Limberg, L. Zhao, G. Frenking and M. Driess, Stabilizing Monoatomic Two-Coordinate Bismuth(I) and Bismuth(II) Using a Redox Noninnocent Bis(germylene) Ligand, *J. Am. Chem. Soc.*, 2024, **146**, 6025–6036.

110 K. L. Deuter, D. J.-J. Balaba, M. Linseis and R. F. Winter, Room-Temperature Near-Infrared Phosphorescence of a Bismuthinidene N,C,N Pincer Complex, *Chem. Commun.*, 2025, **61**, 3548–3551.

111 M. Olaru, D. Duvinage, E. Lork, S. Mebs and J. Beckmann, Heavy Carbene Analogues: Donor-Free Bismuthenium and Stibenium Ions, *Angew. Chem., Int. Ed.*, 2018, **57**, 10080–10084.

112 V. Stavila, R. L. Davidovich, A. Gulea and K. H. Whitmire, Bismuth(III) complexes with aminopolycarboxylate and polyaminopolycarboxylate ligands: Chemistry and structure, *Coord. Chem. Rev.*, 2006, **250**, 2782–2810.

113 A. C. Marwitz, A. D. Nicholas, L. M. Breuer, J. A. Bertke and K. E. Knope, Harnessing Bismuth Coordination Chemistry to Achieve Bright, Long-Lived Organic Phosphorescence, *Inorg. Chem.*, 2021, **60**, 16840–16851.

114 J. I. Musher, The Chemistry of Hypervalent Molecules, *Angew. Chem., Int. Ed. Engl.*, 1969, **8**, 54–68.

115 V. V. Sharutin, A. I. Poddel'sky and O. K. Sharutina, Organic Compounds of Bismuth: Synthesis, Structure, and Applications, *Russ. J. Coord. Chem.*, 2021, **47**, 791–860.

116 P. S. Bagus, Y. S. Lee and K. S. Pitzer, Effects of relativity and of the lanthanide contraction on the atoms from hafnium to bismuth, *Chem. Phys. Lett.*, 1975, **33**, 408–411.

117 H. Nikol and A. Vogler, Photoluminescence of Antimony (III) and Bismuth(III) Chloride Complexes in Solution, *J. Am. Chem. Soc.*, 1991, **113**, 8988–8990.

118 L. A. Maurer, O. M. Pearce, F. D. R. Maharaj, N. L. Brown, C. K. Amador, N. H. Damrauer and M. P. Marshak, Open for Bismuth: Main Group Metal-to-Ligand Charge Transfer, *Inorg. Chem.*, 2021, **60**, 10137–10146.

119 J.-C. Jin, Y.-P. Lin, Y.-H. Wu, L.-K. Gong, N.-N. Shen, Y. Song, W. Ma, Z.-Z. Zhang, K.-Z. Du and X.-Y. Huang, Long lifetime phosphorescence and X-ray scintillation of chlorobismuthate hybrids incorporating ionic liquid cations, *J. Mater. Chem. C*, 2021, **9**, 1814–1821.

120 S. Pavlidis, E. W. Fischer, A. Opis-Basilio, A. Bera, A. Guilherme Buzanich, M. Álvarez-Sánchez, S. Wittek, F. Emmerling, K. Ray, M. Roemelt and J. Abbenseth, Ambiphilic Reactivity and Switchable Methyl Transfer at a T-Shaped Bi(NNN) Complex Enabled by a Redox-Active Pincer Ligand, *J. Am. Chem. Soc.*, 2026, **148**, 2683–2692.

121 P. Coburger, A. G. Buzanich, F. Emmerling and J. Abbenseth, Combining geometric constraint and redox non-innocence within an ambiphilic PBiP pincer ligand, *Chem. Sci.*, 2024, **15**, 6036–6043.

122 K. L. Deuter, F. Kather, M. Linseis, M. Bodensteiner and R. F. Winter, The Emissive and Electrochemical Properties of Hypervalent Pyridine-Dipyrrolide Bismuth Complexes, *Chem. – Eur. J.*, 2024, **31**, e202403761.

123 K. L. Deuter, B. Schneider, K. Jellinek and R. F. Winter, Picturesque Luminescence: The Photophysical and Emissive Properties of Dipyridine Pyrrolide Group 15 Diiodide Complexes, *Z. Anorg. Allg. Chem.*, 2025, **651**, e202500102.

124 M. Geppert, M. Müller, K. J. Scherer, J. Henzler and R. F. Winter, Singlet, Doublet, and Triplet Emissions of Diarylamine-Modified Bismuth Pincer Complexes, *Chem. – Eur. J.*, 2025, **31**, e202500384.

125 W. Ma, L. Xu, S. Zhang, G. Li, T. Ma, B. Rao, M. Zhang and G. He, Phosphorescent Bismoviologens for Electrophosphorochromism and Visible Light-Induced Cross-Dehydrogenative Coupling, *J. Am. Chem. Soc.*, 2021, **143**, 1590–1597.

126 Y. Adachi, S. Terao, Y. Kanematsu and J. Ohshita, Phosphorescence Properties of Boron/Bismuth Hybrid Conjugated Materials, *Chem. – Asian J.*, 2024, **19**, e202301142.

127 J. Ohshita, S. Matsui, R. Yamamoto, T. Mizumo, Y. Ooyama, Y. Harima, T. Murafuji, K. Tao, Y. Kuramochi, T. Kaikoh and H. Higashimura, Synthesis of Dithienobismoles as Novel Phosphorescence Materials, *Organometallics*, 2010, **29**, 3239–3241.

128 N. Shen, Z. Wang, J. Jin, L. Gong, Z. Zhang and X. Huang, Phase transitions and photoluminescence switching in hybrid antimony(III) and bismuth(III) halides, *CrystEngComm*, 2020, **22**, 3395–3405.

129 M. Li and Z. Xia, Recent progress of zero-dimensional luminescent metal halides, *Chem. Soc. Rev.*, 2021, **50**, 2626–2662.

130 S. Wang, H. Zhu, M. Sheng, B. Shao, Y. He, Z. Liu and G. Zhou, Advances of Low-Dimensional Organic-Inorganic Hybrid Metal Halide Luminescent Materials: A Review, *Crystals*, 2025, **15**, 364.

131 X. Chen, M. Jia, W. Xu, G. Pan, J. Zhu, Y. Tian, D. Wu, X. Li and Z. Shi, Recent Progress and Challenges of Bismuth-Based Halide Perovskites for Emerging Optoelectronic Applications, *Adv. Opt. Mater.*, 2023, **11**, 2202153.

132 S. Attique, N. Ali, S. Ali, R. Khatoon, N. Li, A. Khesro, S. Rauf, S. Yang and H. Wu, A Potential Checkmate to Lead: Bismuth in Organometal Halide Perovskites, Structure, Properties, and Applications, *Adv. Sci.*, 2020, **7**, 1903143.

133 J. Heine, B. Peerless, S. Dehnen and C. Lichtenberg, Charge Makes a Difference: Molecular Ionic Bismuth Compounds, *Angew. Chem., Int. Ed.*, 2023, **62**, e202218771.

134 A. M. Goforth, M. A. Tershansy, M. D. Smith, L. Peterson Jr, J. G. Kelley, W. J. I. DeBenedetti and H.-C. zur Loye, Structural Diversity and Thermochromic Properties of Iodobismuthate Materials Containing d-Metal Coordination Cations: Observation of a High Symmetry $[Bi_3I_{11}]^{2-}$ Anion and of Isolated I^- Anions, *J. Am. Chem. Soc.*, 2011, **133**, 603–612.

135 G. Li, P. Hao, J. Shen, T. Yu, H. Li and Y. Fu, Bipyridyltriazolium Chlorobismuthate with Thermo-/Photochromic and Photoluminescent Switching Behaviors Based on ET and CT, *Inorg. Chem.*, 2016, **55**, 11342–11347.

136 Y. Kang, D. Song, H. Schmider and S. Wang, Novel Blue Phosphorescent Group 15 Compounds MR_3 (M = P, Sb, Bi; R = *p* -(N -7-Azaindolyl)phenyl), *Organometallics*, 2002, **21**, 2413–2421.

137 R. C. Smith, M. J. Earl and J. D. Protasiewicz, Synthesis and photoluminescent properties of a series of pnictogen-centered chromophores, *Inorg. Chim. Acta*, 2004, **357**, 4139–4143.

138 E. J. Lee, J. S. Hong, T. Kim, Y. Kang and E. M. Han, Synthesis and Structural Characterization of Main Group 15 Organometallics R_3M and $R(Ph)_2P(=N\text{-}Ar)$(M = P, Sb, Bi; R = phenanthrenyl; Ar = 2,6- $^{i}Pr_2$-C_6H_3), *Bull. Korean Chem. Soc.*, 2005, **26**, 1946–1952.

139 Y. Matano, T. Shinokura, O. Yoshikawa and H. Imahori, Triaryl(1-pyrenyl)bismuthonium Salts: Efficient Photoinitiators for Cationic Polymerization of Oxiranes and a Vinyl Ether, *Org. Lett.*, 2008, **10**, 2167–2170.

140 K. Behm, J. B. Essner, C. L. Barnes, G. A. Baker and J. R. Walensky, Synthesis and fluorescence spectroscopy of tris(pyrenyl)pnictogen compounds, *Dalton Trans.*, 2017, **46**, 10867–10875.

141 H. Amarne, W. Helal and S. Wang, Synthesis, structure and density functional theory calculations of a novel photoluminescent trisarylborane-bismuth(III) complex, *Luminescence*, 2019, **34**, 731–738.

142 M. Geppert, M. Müller, M. Linseis and R. F. Winter, Room-temperature phosphorescence and static excimer excitation of pyrene-modified (NCN) pincer bismuth complexes, *Dalton Trans.*, 2025, **54**, 1779–1783.

143 R. Inaba, K. Oka, T. Iwami, Y. Miyake, K. Tajima, H. Imoto and K. Naka, Systematic Study of Pnictogen-Fused Heterofluorenes, *Inorg. Chem.*, 2022, **61**, 7318–7326.

144 S. M. Parke, M. A. B. Narreto, E. Hupf, R. McDonald, M. J. Ferguson, F. A. Hegmann and E. Rivard, Understanding the Origin of Phosphorescence in Bismoles: A Synthetic and Computational Study, *Inorg. Chem.*, 2018, **57**, 7536–7549.

145 Y. Morisaki, K. Ohashi, H.-S. Na and Y. Chujo, First synthesis of the bismole-containing conjugated polymer, *J. Polym. Sci., Part A: Polym. Chem.*, 2006, **44**, 4857–4863.

146 T. Hirayama, A. Mukaimine, K. Nishigaki, H. Tsuboi, S. Hirosawa, K. Okuda, M. Ebihara and H. Nagasawa, Bismuth-rhodamine: a new red light-excitable photosensitizer, *Dalton Trans.*, 2017, **46**, 15991–15995.

147 A. Mukaimine, T. Hirayama and H. Nagasawa, Asymmetric bismuth-rhodamines as an activatable fluorogenic photosensitizer, *Org. Biomol. Chem.*, 2021, **19**, 3611–3619.

148 J. Ohshita, K. Yamaji, Y. Ooyama, Y. Adachi, M. Nakamura and S. Watase, Synthesis, Properties, and Complex Formation of Antimony- and Bismuth-Bridged Bipyridyls, *Organometallics*, 2019, **38**, 1516–1523.

149 S. Ito, M. Gon and K. Tanaka, Effects of Heavy p-Block Elements on Photophysical Properties of π-Conjugated Complexes and Organoelement Compounds, *Eur. J. Inorg. Chem.*, 2024, **27**, e202400180.

150 S. M. Parke, M. P. Boone and E. Rivard, Marriage of heavy main group elements with π-conjugated materials for optoelectronic applications, *Chem. Commun.*, 2016, **52**, 9485–9505.

151 S. M. Parke, M. A. B. Narreto, E. Hupf, M. Robert, M. J. Ferguson, F. A. Hegmann and E. Rivard, Understanding the Origin of Phosphorescence in Bismoles: A Synthetic and Computational Study, *Inorg. Chem.*, 2018, **57**, 7536–7549.

152 S. N. Davydov, A. N. Rodionov, D. N. Shigorin, O. P. Syutkina and T. L. Krasnova, Electronic spectra and structure of fluorene derivatives of Group IVA-VIA elements, *Zh. Fiz. Khim.*, 1980, **54**, 506–508.

153 V. A. Godik, S. N. Davydov, A. N. Rodionov and D. N. Shogorin, Deactivation of electronically excited states of heteroaromatic derivatives of the fluorene and phenyl series, *Zh. Fiz. Khim.*, 1997, **71**, 1431–1435.

154 S. N. Davydov, A. N. Rodionov, D. N. Shigorin, O. P. Syutkina and T. L. Krasnova, Spectral studies of triplet states of organoelemental derivatives of fluorene, *Zh. Fiz. Khim.*, 1981, **55**, 784–787.

155 H. Yersin and U. Monkowius, Thermally Activated Delayed Fluorescence and Beyond. Photophysics and Material Design Strategies, *Adv. Photonics Res.*, 2025, **6**, 2400111.

156 Y. Zhang, J. L. Petersen and C. Milsmann, A Luminescent Zirconium(IV) Complex as a Molecular Photosensitizer for Visible Light Photoredox Catalysis, *J. Am. Chem. Soc.*, 2016, **138**, 13115–13118.

157 A. S. Gowda, T. S. Lee, M. C. Rosko, J. L. Petersen, F. N. Castellano and C. Milsmann, Long-Lived Photoluminescence of Molecular Group 14 Compounds through Thermally Activated Delayed Fluorescence, *Inorg. Chem.*, 2022, **61**, 7338–7348.

158 D. C. Bhatnagar and L. S. Forster, The luminescence of oxines and metal oxinates, *Spectrochim. Acta*, 1965, **21**, 1803–1807.

159 R. Ballardini, G. Varani, M. T. Indelli and F. Scandola, Phosphorescent 8-quinolinol metal chelates. Excited-state properties and redox behavior, *Inorg. Chem.*, 1986, **25**, 3858–3865.

160 P. J. Han, A. L. Rheingold and W. C. Trogler, Luminescent Tris(8-hydroxyquinolates) of Bismuth(III), *Inorg. Chem.*, 2013, **52**, 12033–12045.

161 K. Tanimura, M. Gon and K. Tanaka, Effects of Hypervalent Bismuth on Electronic Properties of the Azobenzene Tridentate Ligand and Roles of Lewis Acidity in Controlling Optical Properties, *Inorg. Chem.*, 2023, **62**, 4590–4597.

162 M. Imran, B. Neumann, H.-G. Stammler, U. Monkowius, M. Ertl and N. W. Mitzel, The versatile behaviour of a novel Janus scorpionate ligand towards sodium, potassium and bismuth(III) ions, *Dalton Trans.*, 2013, **42**, 15785–15795.

163 M. Imran, A. Mix, B. Neumann, H.-G. Stammler, U. Monkowius, P. Bleckenwegner and N. W. Mitzel, Boron-centered soft ligands based on tetrazole units and their complexes with sodium, potassium and bismuth ions, *Dalton Trans.*, 2014, **43**, 14737–14748.

164 M. Imran, A. Mix, B. Neumann, H.-G. Stammler, U. Monkowius, P. Bleckenwegner and N. W. Mitzel, Synthesis, structural and photo-physical studies of bismuth(III) complexes with Janus scorpionate and co-ligands, *Dalton Trans.*, 2014, **43**, 10956–10968.

165 M. Imran, B. Neumann, H.-G. Stammler, U. Monkowius, M. Ertl and N. W. Mitzel, Borate-based ligands with two soft heterocycle/thione groups and their sodium and bismuth complexes, *Dalton Trans.*, 2014, **43**, 1267–1278.

166 J.-C. Jin, Y.-P. Lin, L.-F. Lin, C. Xiao, Y. Song, N.-N. Shen, L.-K. Gong, Z.-Z. Zhang, K.-Z. Du and X.-Y. Huang, 2,2′-Bipyridyl-1,1′-dioxide based bismuth(III) bromide hybrids: studies on crystal structure and luminescence, *CrystEngComm*, 2021, **23**, 3744–3752.

167 N. Shen, J. Li, Z. Wu, B. Hu, C. Cheng, Z. Wang, L. Gong and X. Huang, α- and β-[Bmim][$BiCl_4$(2,2′-bpy)]: Two Polymorphic Bismuth-Containing Ionic Liquids with Crystallization-Induced Phosphorescence, *Chem. – Eur. J.*, 2017, **23**, 15795–15804.

168 A. C. Marwitz, A. D. Nicholas, R. T. Magar, A. K. Dutta, J. Swanson, T. Hartman, J. A. Bertke, J. J. Rack, L. G. Jacobsohn and K. E. Knope, Back in bismuth: controlling triplet energy transfer, phosphorescence, and radioluminescence via supramolecular interactions, *J. Mater. Chem. C*, 2023, **11**, 14848–14864.

169 A. Loudet and K. Burgess, BODIPY Dyes and Their Derivatives: Syntheses and Spectroscopic Properties, *Chem. Rev.*, 2007, **107**, 4891–4932.

170 P. De Bonfils, L. Péault, P. Nun and V. Coeffard, State of the Art of Bodipy-Based Photocatalysts in Organic Synthesis, *Eur. J. Org. Chem.*, 2021, 1809–1824.

171 C. M. Lemon, Corrole photochemistry, *Pure Appl. Chem.*, 2020, **92**, 1901–1919.

172 A. Korzun, S. Crespi, C. Golz and A. Bismuto, Replacing the BO in BODIPY: unlocking the path to SBDIPY and BIDIPY chromophores, *Chem. Sci.*, 2023, **14**, 6579–6584.

173 C. Liu, Y. Dai, Q. Han, C. Liu and Y. Su, Crystalline heaviest pnictogen-dipyrromethenes: isolation, characterization, and reactivity, *Chem. Commun.*, 2023, **59**, 2161–2164.

174 Z. Valicsek, O. Horváth and K. Patonay, Formation, photophysical and photochemical properties of water-soluble bismuth(III) porphyrins: The role of the charge and structure, *J. Photochem. Photobiol.*, 2011, **226**, 23–35.

175 L. M. Reith, M. Stiftinger, U. Monkowius, G. Knör and W. Schoefberger, Synthesis and Characterization of a Stable Bismuth(III) A3−Corrole, *Inorg. Chem.*, 2011, **50**, 6788–6797.

176 T. Agou, S. Kuroiwa, R. Moriyama, T. Kuroda, K. Kubo, H. Fukumoto, M. Morita, R. Inoue and T. Nabeshima, Synthesis and structural characterization of Sb(III) and Bi(III) complexes with an N_2O_2-type tetradentate dipyrrin ligand, *Chem. Commun.*, 2025, **61**, 7141–7144.

177 A. Korzun, M. J. McKee, H. Neugebauer, O. Green, G. Schnakenburg, S. Grimme, N. Kornienko and A. Bismuto, Antimony and Bismuth Complexes as Visible Light Photosensitizers in Catalytic Oxidation Reactions, *Inorg. Chem.*, 2025, **64**, 15667–15679.

178 K. L. Deuter, K. Vollmar, J. Rieser, M. Linseis and R. F. Winter, The influence of charge transfer on the emissive properties of pyridine dipyrrolide bismuth complexes, *Dalton Trans.*, 2025, **54**, 9921–9929.

179 M. Gouterman, Spectra of porphyrins, *J. Mol. Spectrosc.*, 1961, **6**, 138–163.

180 Z. Valicsek and O. Horváth, Application of the electronic spectra of porphyrins for analytical purposes: The effects of metal ions and structural distortions, *Microchem. J.*, 2013, **107**, 47–62.

181 B. Boitrel, Z. Halime, S. Balieu and M. Lachkar, The coordination of bismuth by porphyrins, *C. R. Chim.*, 2007, **10**, 583–589.

182 L. Michaudet, D. Fasseur, R. Guilard, Z. Ou, K. M. Kadish, S. Dahaoui and C. Lecomte, Synthesis, characterization and electrochemistry of bismuth porphyrins. X-ray crystal structure of (OEP)Bi(SO_3CF_3), *J. Porphyrins Phthalocyanines*, 2000, **4**, 261–270.

183 Q. Mao, P. K. Das, S. L. Gac, B. Boitrel, V. Dorcet, K. Oohora, T. Hayashi and H. Kitagishi, Functional Myoglobin Model Composed of a Strapped Porphyrin/Cyclodextrin Supramolecular Complex with an Overhanging COOH That Increases O_2/CO Binding Selectivity in Aqueous Solution, *Inorg. Chem.*, 2021, **60**, 12392–12404.

184 B. Boitrel, M. Breede, P. J. Brothers, M. Hodgson, L. Michaudet, C. E. F. Rickard and N. Al Salim, Bismuth porphyrin complexes: syntheses and structural studies, *Dalton Trans.*, 2003, 1803–1807, DOI: **10.1039/B210318D**.

185 I. S. Schomberg-Sanchez, W. A. Janusz and C. M. Lemon, Beyond BODIPY: dipyrrin complexes of *P*-block elements, *J. Coord. Chem.*, 2025, 1–54, DOI: **10.1080/00958972.2025.2539945**.

186 J. Karges, O. Blacque and G. Gasser, Metal dipyrrin complexes as potential photosensitizers for photodynamic therapy, *Inorg. Chim. Acta*, 2020, **505**, 119482.

187 R. Prieto-Montero, A. Prieto-Castañeda, R. Sola-Llano, A. R. Agarrabeitia, D. García-Fresnadillo, I. López-Arbeloa, A. Villanueva, M. J. Ortiz, S. de la Moya and V. Martínez-Martínez, Exploring BODIPY Derivatives as Singlet Oxygen Photosensitizers for PDT, *Photochem. Photobiol.*, 2020, **96**, 458–477.

188 A. Stamoulis, M. Mato, P. C. Bruzzese, M. Leutzsch, A. Cadranel, M. Gil-Sepulcre, F. Neese and J. Cornella, Red-Light-Active N,C,N-Pincer Bismuthinidene: Excited State Dynamics and Mechanism of Oxidative Addition into Aryl Iodides, *J. Am. Chem. Soc.*, 2025, **147**, 6037–6048.

189 J.-C. G. Bünzli, On the design of highly luminescent lanthanide complexes, *Coord. Chem. Rev.*, 2015, **293–294**, 19–47.

190 A. C. Marwitz, A. K. Dutta, R. L. Conner, L. A. Sanz, L. G. Jacobsohn and K. E. Knope, Unlocking Arene Phosphorescence in Bismuth–Organic Materials, *Inorg. Chem.*, 2024, **63**, 11053–11062.

191 A. Thirumurugan, W. Li and A. K. Cheetham, Bismuth 2,6-pyridinedicarboxylates: Assembly of molecular units into coordination polymers, CO_2 sorption and photoluminescence, *Dalton Trans.*, 2012, **41**, 4126–4134.

192 N. Shen, J. Li, G. Li, B. Hu, J. Li, T. Liu, L. Gong, F. Huang, Z. Wang and X. Huang, Designing Polymorphic Bi^{3+}-Containing Ionic Liquids for Stimuli-Responsive Luminescent Materials, *Inorg. Chem.*, 2019, **58**, 8079–8085.

193 J.-C. Jin, N.-N. Shen, Y.-P. Lin, L.-K. Gong, H.-Y. Tong, K.-Z. Du and X.-Y. Huang, Modulation of the Structure and Photoluminescence of Bismuth(III) Chloride Hybrids by Altering the Ionic-Liquid Cations, *Inorg. Chem.*, 2020, **59**, 13465–13472.

194 J.-C. Jin, Y.-P. Lin, D.-Y. Chen, B.-Y. Lin, T.-H. Zhuang, W. Ma, L.-K. Gong, K.-Z. Du, J. Jiang and X.-Y. Huang, X-ray scintillation and photoluminescence of isomorphic ionic bismuth halides with $[Amim]^+$ or $[Ammim]^+$ cations, *Inorg. Chem. Front.*, 2021, **8**, 4474–4481.

195 T.-H. Zhuang, Y.-M. Lin, H.-W. Lin, Y.-L. Guo, Z.-W. Li, K.-Z. Du, Z.-P. Wang and X.-Y. Huang, Luminescence Enhancement and Temperature Sensing Properties of Hybrid Bismuth Halides Achieved via Tuning Organic Cations, *Molecules*, 2023, **28**, 2380.

196 O. Toma, N. Mercier, M. Allain, A. Forni, F. Meinardi and C. Botta, Aggregation induced phosphorescent N-oxyde-2,2′-bipyridine bismuth complexes and polymorphism-dependent emission, *Dalton Trans.*, 2015, **44**, 14589–14593.

197 O. Toma, N. Mercier and C. Botta, N-Methyl-4,4′-bipyridinium and N-Methyl-N′-oxide-4,4′-bipyridinium Bismuth Complexes – Photochromism and Photoluminescence in the Solid State, *Eur. J. Inorg. Chem.*, 2013, 1113–1117.

198 O. Toma, N. Mercier, M. Allain and C. Botta, Protonated N-oxide-4,4′-bipyridine: from luminescent Bi^{III} complexes to hybrids based on H-bonded dimers or H-bonded open 2D square supramolecular networks, *CrystEngComm*, 2013, **15**, 8565–8571.

199 O. Toma, M. Allain, F. Meinardi, A. Forni, C. Botta and N. Mercier, Bismuth-Based Coordination Polymers with Efficient Aggregation-Induced Phosphorescence and Reversible Mechanochromic Luminescence, *Angew. Chem., Int. Ed.*, 2016, **55**, 7998–8002.

200 O. Toma, N. Mercier, M. Allain, F. Meinardi, A. Forni and C. Botta, Mechanochromic Luminescence of N,N′-Dioxide-4,4′-bipyridine Bismuth Coordination Polymers, *Cryst. Growth Des.*, 2020, **20**, 7658–7666.

201 T. Zhuang, Y. Lin, J. Jin, Z. Deng, Y. Peng, L. Gong, Z. Wang, K. Du and X. Huang, A Mechanochemically Synthesized Hybrid Bismuth Halide as Highly Efficient Red Phosphor for Blue Chip-Based WLED, *Adv. Opt. Mater.*, 2023, **11**, 2202951.

202 D.-D. Huang, A. Ablez, T.-H. Zhuang, H.-W. Lin, Z.-H. Deng, K.-Z. Du, Z.-P. Wang and X.-Y. Huang, A Bi (iii)-based halide with near-unity photoluminescence quantum yield as a blue-light-excited red phosphor for WLEDs, *J. Mater. Chem. C*, 2025, **13**, 7276–7281.

203 K. V. Borysova, J. R. Sorg, E. A. Mikhalyova, K. Oberst, C. Würtele and K. Müller-Buschbaum, Bismuth trihalide based coordination polymers with the N-donor cyanopyridine as source for charge transfer based luminescence, *Z. Anorg. Allg. Chem.*, 2023, **649**, e202300131.

204 J. R. Sorg, T. Schneider, L. Wohlfarth, T. C. Schäfer, A. Sedykh and K. Müller-Buschbaum, Sb- and Bi-based coordination polymers with N-donor ligands with and without lone-pair effects and their photoluminescence properties, *Dalton Trans.*, 2020, **49**, 4904–4913.

205 J. R. Sorg, T. Wehner, P. R. Matthes, R. Sure, S. Grimme, J. Heine and K. Müller-Buschbaum, Bismuth as a versatile cation for luminescence in coordination polymers from BiX_3/4,4′-bipy: understanding of photophysics by

quantum chemical calculations and structural parallels to lanthanides, *Dalton Trans.*, 2018, **47**, 7669–7681.

206 A. K. Adcock, A. C. Marwitz, L. A. Sanz, R. L. Ayscue, J. A. Bertke and K. E. Knope, Synthesis, structural characterization, and luminescence properties of heteroleptic bismuth-organic compounds, *CrystEngComm*, 2021, **23**, 8183–8197.

207 R. L. Ayscue, V. Vallet, J. A. Bertke, F. Réal and K. E. Knope, Structure–Property Relationships in Photoluminescent Bismuth Halide Organic Hybrid Materials, *Inorg. Chem.*, 2021, **60**, 9727–9744.

208 Y. Chen, J. W. Y. Lam, R. T. K. Kwok, B. Liu and B. Z. Tang, Aggregation-induced emission: fundamental understanding and future developments, *Mater. Horiz.*, 2019, **6**, 428–433.

209 J. Xu, M. H. Chua and B. Z. Tang, *Aggregation-Induced Emission (AIE): A Practical Guide*, Elsevier Science, Amsterdam, the Netherlands, 1 edn, 2022.

210 C. Zhu, S. Pang, J. Xu, L. Jia, F. Xu, J. Mei, A. Qin, J. Sun, J. Ji and B. Tang, Aggregation-induced emission of tetraphenylethene derivative as a fluorescence method for probing the assembling/disassembling of amphiphilic molecules, *Analyst*, 2011, **136**, 3343–3348.

211 N. N. Greenwood and A. Earnshaw, *Chemistry of the Elements*, Butterworth-Heinemann, Oxford, 2nd edn, 1997.